UC Irvine

UC Irvine Electronic Theses and Dissertations

Title

Exploring Mitochondrial Activities in Murine Brain as a Potential Mechanism for Normal Tissue Protection by FLASH Radiotherapy

Permalink

https://escholarship.org/uc/item/0hb4407b

Author

Kim, Rachel Youn Kyung

Publication Date

2023

Copyright Information

This work is made available under the terms of a Creative Commons Attribution-NoDerivatives License, available at https://creativecommons.org/licenses/by-nd/4.0/

Peer reviewed|Thesis/dissertation

eScholarship.org Powered by the California Digital Library
University of California

UNIVERSITY OF CALIFORNIA,
IRVINE

Exploring Mitochondrial Activities in Murine Brain as a Potential Mechanism for Normal Tissue Protection by FLASH Radiotherapy

A THESIS

Submitted in partial satisfaction of the requirement
for the degree of

MASTER OF SCIENCE

in Environmental Health Sciences

by

Rachel Youn Kyung Kim

Thesis Committee:
Professor Charles L. Limoli, Chair
Associate Professor Masashi Kitazawa
Professor Ulrike Luderer

2023

© 2023 Rachel Youn Kyung Kim

DEDICATION

For my parents –

whom I have been blessed to call such wonderful and honorable individuals,

my father and mother

“And God said, ‘Let there be Light,’ and there was Light.”
Genesis 1:3

TABLE OF CONTENTS

LIST OF FIGURES

LIST OF TABLES

ACKNOWLEDGEMENTS

First and foremost, I extend my deepest appreciation to Professor Charles Limoli for welcoming me into the lab and engaging me in intriguing and intensely thought-provoking conversations. Your guidance and encouragement have helped me grow as a more resilient student and individual.

I would like to express my gratitude to Professors Masashi Kitazawa and Ulrike Luderer, not only for serving as my thesis committee members but also for delivering inspiring lectures and offering warm advice throughout my master's program. Your knowledge and guidance have been invaluable.

I thank our collaborators at Lausanne University Hospital, Switzerland (CHUV), and at Stanford University, CA, for irradiating our samples.

A special thank you goes to all the members of the Limoli Lab – Dr. Janet Baulch, for your unwavering support for the team day in and day out. Ning Ru and Olivia Drayson, for the fun moments we shared running our assays. To now-Dr. Barrett Allen, thank you for training me in the lab when I first arrived and being the dependable handyman who fixed our plate reader and Li-Cor machine in very critical moments. Richard Zhang, for your support in preparing samples for Raman spectroscopy and your insights on statistics and choosing the right marker to test.

I am indebted to Dr. Scott Bartell and Quinton Ng for their assistance with statistical analyses, despite their busy schedules. Thank you so much. To Dr. Junghwa Kim and her graduate writing class, thank you for your support in finalizing my thesis draft.

I would also like to extend my appreciation to the members of the Acharya lab – Dr. Munjal Acharya, for your support, and particularly Sanad El Khatib and Manal Usmani, for your friendship.

Thank all my EHS friends, Keira Truong, Xiaomeng Lin, Joan Vu, and Shayna Simona, for all the good food and good laughs that kept me going. Finally, many thanks to my parents, Dr. Hyun Kim, DDS, and Jung Kang, for all your love and support, which has let me stay curious as I walk my learning journey.

ABSTRACT OF THE THESIS

Exploring Mitochondrial Activities in Murine Brain as a

Potential Mechanism for Normal Tissue Protection by FLASH Radiotherapy

by

Rachel Youn Kyung Kim

Master of Science in Environmental Health Sciences

University of California, Irvine, 2023

Professor Charles L. Limoli, Chair

Purpose: FLASH radiotherapy's enhanced normal tissue protective effect without compromising cancer treatment efficacy has stimulated investigations exploring its mechanisms. To this date, mitochondrial endpoints after FLASH radiotherapy have not been explored. This master's thesis aims to narrate the *in vivo* accounts of the normal tissue-sparing FLASH effect observed across organ systems and report the findings in ATP production and mitochondrial dynamics in the murine brain as possible explanations for the FLASH effect.
Methods: Two cohorts received 10 Gy whole-brain FLASH and conventional dose rate irradiations at two different facilities. Stanford FLASH dose rate per pulse was 5.3×10^5 Gy/s, with mean dose rate of 225 Gy/s. CHUV FLASH dose rate was 5.6×10^6 Gy/s, where a single 1.8 microsecond pulse was used to administer the total dose. The conventional dose rate was 0.1 Gy/s at both locations. At 4 months post-irradiation, ATP concentration and OPA-1 mitochondrial fusion protein levels were measured from the hippocampus and frontal cortex tissues and compared across the treatment groups via one-way ANOVA and Pearson's correlation analyses.
Results: The hippocampus tissues from Stanford FLASH- and CHUV conventional-irradiated groups had significantly different associations between long and short OPA-1 isoforms compared to the control ($p=0.005$ and $p=0.012$, respectively). Although the strengths of associations in the hippocampal tissues were weaker than their cortex counterparts across the cohorts, only the Stanford CONV and FLASH irradiated groups showed significant and marginally significant differences between the brain regions ($p=0.0496$ and 0.057, respectively). These differences indicate that the mitochondrial dynamics may be dysregulated in the hippocampus at 4 months post-irradiation. The individual levels of ATP, L-OPA1, S-OPA1, and the ratios of isoforms did not significantly differ across the treatment groups.
Conclusion: Despite the low sample size ($n \leq 12$), there may be evidence for dysregulated mitochondrial dynamics in the hippocampus after CONV and FLASH irradiations at a late time point. Further study should confirm the radiation-induced effect on mitochondrial physiology through more refined tests.

CHAPTER 1.

Introduction and Background of Conventional and FLASH Radiotherapy

Cancer is a complex, multifactorial disease that most commonly occurs in the population aged over 50 years (1). Yet, diagnosis in younger adults has been rising in the U.S., a phenomenon referred to as the early-onset cancer epidemic (1). Cancer incidence rates, regardless of age and sex, have continuously increased since the Surveillance, Epidemiology, and End Results Program (SEER) began collecting U.S. statistics in 1975 (2). Although cancer mortality rates have been declining post-1990s – partially accounted for by decreased smoking and improved cancer detection and treatment outcomes – cancer has yet to be conquered. Treatment strategies also need to reduce unintended adverse consequences in survivors (1, 2).

Along with surgery and chemotherapy, radiation therapy is a common form of treatment that 60% of cancer patients undergo in the U.S. (3). Radiation therapy is the least invasive but not without adverse effects that vary by treatment location. This thesis aims to discuss unconventional FLASH radiotherapy (FLASH RT), which has the potential to change the current landscape of radiation therapy by reducing radiation-induced injuries, thereby preserving the quality of life in cancer survivors.

Conventional Radiotherapy

Radiotherapy is a frontline cancer treatment used to manage over 50% of patients diagnosed with various malignancies by taking advantage of the cytotoxic characteristics of ionizing radiation (4). There is external and internal radiotherapy (brachytherapy), but this paper will focus on external beam radiation therapy – hereon, radiotherapy.

Successful radiotherapy must achieve two factors: tumor growth control and the maximal preservation of healthy tissues within the radiation field (5). The former is achieved by exploiting radiation as a potent cytotoxic agent, where ionizing radiation causes lethal DNA double-strand breaks (DSB) in cancer cells. The latter is the dose-limiting factor that relies on precise dose delivery to tumor tissues while limiting the dose to normal tissues as much as possible. Healthy cells generally have a superior recovery potential than cancer cells, but ionizing radiation is toxic to cancerous and normal cells alike (6). Therefore, the therapeutic index is narrow, which means the dose range that can achieve a successful tumor growth control (the therapeutic effect) without injuring the surrounding healthy cells (the toxic effect) is small (5) (figure 1).

Conventional radiotherapy (CONV RT) typically administers 2 Gy daily fractions at dose rates of around 0.01 Gy/s over a few days to weeks until the prescribed total dose has been delivered (7). The dose fractionation regimen takes advantage of superior normal tissue tolerability against radiation compared to cancer via the four Rs of radiotherapy: repair, reassort, repopulate, and reoxygenate (3, 8). Smaller doses over longer times allow cancer cells, typically more hypoxic than normal cells, to redistribute into radio-sensitive stage of cell cycle and reoxygenate, although re-oxygenation is not exploitable in the clinic. Meanwhile, sub-lethally injured normal cells can repair radiolytic damage more efficiently (if only slightly) than cancer cells, providing a survival edge over protracted treatment schedules (6, 8). Regeneration and tissue recovery are thus enhanced in normal tissue vs. cancer, providing a narrow window for enhancing the therapeutic index.

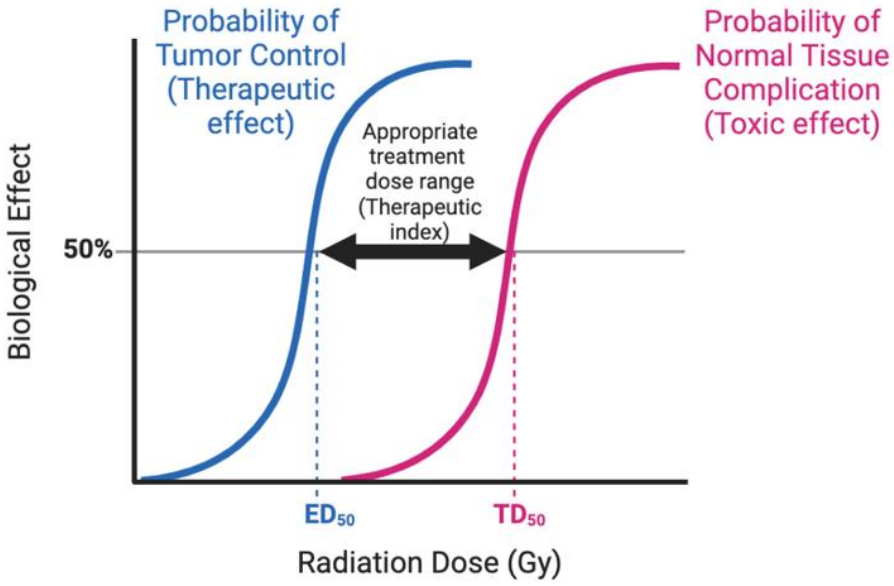

Figure 1. Generalized illustration of the therapeutic window of radiotherapy, depicting the balance between treatment efficacy and normal tissue toxicity (Created with BioRender.com)

Since the first utilization of radiation in oncology in the late 19th century, advancements in precision imaging and beam delivery techniques have decreased burdens on healthy tissues (5, 6, 9, 10, 11). Instead of administering radiation to the approximated region of the body, clinicians visualize and specifically target the tumor bed via 3D conformal RT and image-guided RT. However, these technological advancements have widened the therapeutic window incrementally, and CONV RT still has limitations to be addressed (12). For example, while dose fractionation allows for normal tissue sublethal damage repair, CONV RT has an inherent problem of intra-fraction organ motion, which results in radiation inevitably depositing in healthy tissues during a few minutes of treatment (11). Further, radiation-induced toxicity that is volume-dependent confines treatments to a suboptimal dose range for tumor growth control compromising curative intent and beneficial outcomes (9). The focus of the remainder of this thesis will be to expand and

explore how a new radiation modality overcomes many of the long-standing limitations of standard-of-care radiotherapy, a modality termed FLASH radiotherapy.

FLASH Radiotherapy

Much effort in improving treatment outcomes has focused on minimizing normal tissue irradiation by enhancing tumor visualizing techniques (6, 13). Meanwhile, the biological effects of dose rate had remained relatively under-investigated since the 1980s until 2014, when a team of scientists from France explored the effect of single-dose radiation delivered in a fraction of a second to normal or cancerous lung tissues (9, 10). While this method evades the intra-fraction organ motion during CONV RT, administering a total dose under a second rather than a few minutes went against conventional wisdom. Reasons for this are simple, as a preponderance of literature had found benefits at lower dose rates due to the superposition of DNA damage repair and dose delivery that ameliorated adverse radiation-induced outcomes (13). Thus, to the field's surprise, was the finding that ultrahigh dose rate (UHDR) radiation at ≥40 Gy/s significantly decreased normal tissue toxicity in murine lungs more than CONV RT. Even more intriguing, tumor growth control remained equally as efficacious at FLASH and CONV dose rates. As a result, normal tissue and tumor cells exhibited a differential response to UHDR irradiation in a way that would widen the therapeutic index of radiotherapy. Henceforth, UHDR irradiation was named FLASH radiotherapy, and the enhanced normal tissue protection and equivalent anti-tumor efficacy was named the FLASH effect (9).

There are a few historical accounts of such reduced biological effectiveness – or reduced toxicity – via UHDR irradiation. An experiment from 1959 showed increased

radioresistance in bacteria irradiated with 3-6 x10^9 Gy/min compared to conventional dose rates of 0.5-20 Gy/min (5, 14). In 1974, Field and Bewley irradiated rat hind limbs with a 30 Gy single-dose electron beam. They observed that 66.67 Gy/s caused no deformity while 0.03 and 1 Gy/s dose rates resulted in the deformity score of 3 at six months post-irradiation (post-IR) (15). The highest dose rate irradiation resulted in superior normal skin tissue protection at both acute (7-35 days) and late (5-23 weeks) time points (15).

It was once thought that UHDR could be useful in killing cells regardless of oxygen tension – such as radioresistant tumor cells that are hypoxic – as normoxic and hypoxic cells react similarly to UHDR irradiation (9, 16). However, this interesting phenomenon remained dormant for several decades in the field of radiation oncology because if normal tissue sparing were translated to reduced tumor kill, then no advantage of UHDR radiotherapy would make sense in the clinic (5, 9, 16). It must be noted that another group of researchers explored the efficacy of UHDR proton irradiation on tumor growth control just a few months before this study was published in 2014 (17). However, Favaudon et al. were the first since the 1980s to demonstrate normal tissue protection after UHDR irradiation while also illustrating the detrimental effects on lung cancer cells. The pioneering team revitalized the possibilities of UHDR irradiation to increase the therapeutic index in cancer treatment and revitalized the entire field of radiobiology in so doing (9, 14).

Following the 2014 renaissance paper, numerous studies have investigated the FLASH effect across various species, organs, and tissue types. Current work is evaluating physical, chemical, and biological aspects of FLASH RT to achieve appropriate dose

parameters and survey mechanistic explanations of the FLASH effect. Besides the technological hurdles, defining the critical beam parameters has become increasingly critical as the average dose rate of ≥40 Gy/s soon proved to be too simplistic; the current FLASH dose rate has been narrowed down to “delivering large single doses of radiation (10-20 Gy) at mean dose rates above 100 Gy/s” (18, 19, 20). Furthermore, pulse repetition rate, number and duration of pulses, and total exposure time are important additional physical parameters that should be clearly mentioned in experimental FLASH RT studies (18).

This thesis aims to give a comprehensive overview of experimental studies performed on FLASH RT and compile the knowns to narrow down the mechanisms of the FLASH effect. Chapter 2 summarizes FLASH effects achieved in normal organ types and tumor studies. Chapter 3 discusses mechanistic explanations for the FLASH effect and presents experimental outcomes that assess the impact of FLASH RT on metabolic activities in the murine brain, specifically, steady-state ATP concentrations and mitochondrial fusion activity. We hypothesized that FLASH RT would result in differential mitochondrial activities compared to CONV RT considering the abundance of mitochondria in target organs and their dynamic involvement in cellular activities.

CHAPTER 2.

FLASH Effects Observed by Organ Types

2.1. Normal Lung

The pioneers of FLASH RT performed their first investigation via a dose escalation study. *In vivo* administration of 15 Gy CONV RT (≤0.03 Gy/s) resulted in lung fibrosis, while 17 Gy FLASH RT (≥40 Gy/s) did not (10). Dose escalation ranging from 16 to 30 Gy revealed that adverse effects such as cachexia began to emerge in ≥23 Gy FLASH treatment groups 32 weeks post-irradiation (post-IR). 30 Gy FLASH irradiation caused pulmonary edema and macrophage infiltration, indicating a dose limitation for the dose rate of ≥40 Gy/s. Still, the extent of vascular apoptosis at 30 Gy FLASH RT was comparable to the level caused by a much lower dose of 7.5 Gy CONV RT, which illustrated the superior protective effect of FLASH RT.

The importance of clearly outlining the detailed beam parameters (such as instantaneous dose rate, pulse duration, average dose rate, etc.) was not yet recognized in this initial study of the FLASH RT. *The above details are the synopsis of the first FLASH radiotherapy study published in 2014 by Favaudon et al. (10).*

Stem cells are radiosensitive, and their preservation directly influences the ability to recover from radiation-induced damage in normal tissues post-IR (7). Fouillade et al. explored the effects of FLASH and CONV RT on lung progenitor cells and human fibroblast cell lines via gene expression pathways.

17 Gy electron CONV RT showed significantly increased EdU+ cells in murine lungs, indicating active cell division. In contrast, levels in 17Gy FLASH-irradiated mice did not

statistically differ from that of non-irradiated control (CTL). The tissues were also assessed for acute alterations in gene expression four days post-IR. FLASH RT, unlike CONV RT, did not upregulate proinflammatory pathways or induce senescence and fibrogenesis. Instead, recovery and repair pathways were upregulated. Interestingly, this protective effect was removed in Terc-/- mice with short telomeres. While only 1/8 FLASH irradiated wildtype mice developed fibrosis, 7/8 FLASH and 12/12 CONV RT Terc-/- mice developed fibrosis, opening the door to exploring the genetic factors contributing to deducing the mechanisms of the FLASH effect.

In vitro DNA damage analyses of human lung fibroblast cell lines showed no significant differences in H2AX between FLASH and CONV RT. However, the 53BP1 foci count had significantly increased at three months post-17 Gy CONV RT compared to 1 week, suggesting that CONV irradiated cells continue to accumulate DNA damage as a late response. Multiple markers pointed to superior protection by FLASH RT. Cell senescence indicator SA-b-gal+ clusters were significantly reduced by FLASH RT compared to CONV RT at both four days and four months post-IR; FLASH downregulated proinflammatory factors such as TGFB1, CEBPB, and NF-κB; P63+ basal stem cell population was better salvaged by 4 Gy FLASH than CONV RT at 21 days post-IR; and FLASH reduced EGR1 expression, upregulating hematopoietic stem cells in the AT2 alveolar stem cell population. Because FLASH RT minimizes damage and, in turn, does not require as much stem cell proliferation as CONV irradiated mice, FLASH RT may preserve lung stem cells from exhaustion due to over-replication. FLASH RT may have ranged between 200 and $4x10^7$ Gy/s according to the referenced study for dose rate, but the dose rates for FLASH and CONV RT were not clearly

indicated. The importance of defining beam parameters may not yet have been recognized at the time of this study. *The above details are the synopsis of a 2019 study conducted by Fouillade et al. (7).*

Electrons and low-energy X-rays have low penetrating power but are the most available modalities of radiotherapy. Gao et al. achieved the FLASH effect with murine normal lung tissue and murine breast cancer tissues using 8.2 MeV high-energy X-rays (HEX), the only account other than the brain irradiation study by Montay-Gruel et al. 2018 that used X-rays to induce a FLASH effect.

30 Gy whole-thorax irradiation (WTI) resulted in 90% survival in the FLASH group (1200 Gy/s) 60 days post-IR, which was statistically superior to the 50% survival in the 24 Gy CONV group (0.1 Gy/s). The risk of death by FLASH RT was 81%. Masson special staining of alveolar structures in FLASH irradiated mice showed that the tissues were histologically better intact compared to CONV RT, which induced more alveolar fibrosis. In the equal dose experiment, 30 Gy FLASH had a mean survival day of 120, while 30 Gy CONV had 86 days, and this difference was also statistically significant. Interestingly, this 30 Gy FLASH RT at 1200 Gy/s did not induce noticeable histological changes while the 30 Gy at ≥40 Gy/s from the 2014 study caused massive pulmonary edema (10). Although radiation modalities were different (HEX vs. electrons), the shorter delivery time by Gao et al. was likely the reason for a decreased normal tissue damage. The dose rate aspect of FLASH RT is explored in more detail in the murine brain dose-rate escalation study by Montay-Gruel et al. 2017. *The above details are the synopsis of a 2021 study by Gao et al. (21).*

Normal Lung Irradiation (Gy)	CONV RT	FLASH RT
7.5	Caspase-3 cleavage 1 hr post-IR (10)	-
15	Fibrosis (10)	No fibrosis or inflammatory cascade (10)
16	-	No fibrosis or lesions (10)
17	Fibrosis at 8 wk post-IR (10) Increased EdU+ cells (7)	No fibrosis, inflammation, caspase-3 cleavage (10) No changes in EdU+ cells, inflammation, senescence (7)
20	-	No fibrosis or lesions; some hair depigmentation (10)
23	-	Cachexia 32 weeks post-IR (10)
24	50% survival (21)	-
28	-	No fibrosis; 80% survival 62 d post-IR (10)
30	-	Edema, lesions, macrophage infiltration 24 wk post-IR; caspase-3 cleavage (10); 90% survival (21); lesions and fibrosis; no lesions and fibrosis by 50 and 500 μm microbeam FLASH RT (22)
50	-	lesions and fibrosis; no lesions and fibrosis by 50 and 500 μm microbeam FLASH RT (22)
100	-	Mild fibrosis by 50 and 500 μm microbeam FLASH RT (22)
300	-	No lesions, mild fibrosis by 50 μm microbeam, scarring and fibrosis by 500 μm FLASH RT (22)
600	-	Lesions and mild fibrosis by 50 μm microbeam, scarring and fibrosis by 500 μm FLASH RT (22)

Table 1. Comparisons of normal lung tissue responses after CONV and FLASH dose-rate irradiations by total dose

Wright et al. were the first to describe the effects of a microbeam FLASH RT (FLASH MRT) in rat lungs and compare the differences with classic FLASH RT, which consists of a broader beam (22). 50 and 500 μm FLASH MRT beams were delivered in doses of 50, 100, 300, and 600 Gy. FLASH RT beam width was 1 cm x 1 cm, and 30 and 50 Gy doses were administered. The average dose rate for both types of FLASH irradiation was 1.4×10^4 Gy/s.

30 and 50 Gy FLASH RT resulted in noticeable lesions, while 50% of animals irradiated by 500 μm FLASH MRT showed scarring at the greater, 300 and 600 Gy doses and 50 μm FLASH MRT at 600 Gy. Fibrosis scores were 4 and 5 in FLASH RT, while all doses delivered via 50 μm FLASH MRT resulted in scores under 2, and 500 μm FLASH MRT showed high scores of 4 and 5 at 300 and 600 Gy doses, but a mild score of 1 at 50 and 100 Gy doses. It is remarkable that 50 Gy of 50 μm FLASH MRT did not induce any fibrosis (score = 0), while regular FLASH RT resulted in the score of 5.

The results of this study furthered the possibilities of increasing radiotherapy's therapeutic index via FLASH RT to a greater extent, which would be especially beneficial to the treatments of radiosensitive organs such as lungs and intestines. Future studies should perform tumor control experiments to characterize the treatment efficacy of FLASH MRT. *The above details are the synopsis of a 2021 study by Wright et al. (22).*

2.1.1. Lung Cancer

The first FLASH RT experiments by Favaudon et al. also included a human tumor xenograft study, which revealed the amount of reduction in the relative tumor volume (RTV) of HBCx-12A after 17 Gy CONV and FLASH were statistically indistinguishable (10). For an unknown reason, tumor cells were aloof to the vast difference in the dose rates of CONV and FLASH RT, unlike the responses seen by the normal lung tissues (10).

HEp-2 tumor xenograft irradiated by 15, 20, and 25 Gy FLASH and 19.5 Gy CONV RT showed decreasing RTV proportional to increasing dose, regardless of RT type. It is no surprise that the highest dose of 25 Gy (FLASH RT) resulted in the best tumor growth

control with complete growth control after 40 days post-IR. However, it was remarkable that it did not damage the skin within the radiation field, which demonstrated a potential for improving the therapeutic index via FLASH RT.

The team also performed a dose escalation study using the TC-1 Luc+ orthotopic lung tumors between 13 and 15 Gy CONV and 15, 23, and 28 Gy FLASH. 15 Gy CONV and FLASH RT, again, had a similarly poor tumor control which resulted in 20% survival rates six days post-engraftment of the tumor. 23 and 28 Gy FLASH treatments were more efficient at tumor control. Tumor progression resumed in 80% of the 15 Gy CONV group four to five weeks post-engraftment, with 20% of mice surviving with fibrosis. 28 Gy FLASH had an 80% survival rate, and 70% were free of tumors as well as fibrosis 62 wk post-IR. *The above details are the synopsis of the first FLASH radiotherapy study published in 2014 by Favaudon et al. (10).*

Rama et al. performed one of the few proton FLASH studies on orthotopic Lewis lung carcinoma (LLC) in male and female mice (23). Proton RT is costly and not nearly as available as X-rays and electron RTs. Still, it can penetrate deeper, does not have an exit dose, and some studies have reported reduced long-term gut toxicities, possibly because it allows for significantly reduced dose distributions on normal tissues (24, 25). If the FLASH effect can be achieved regardless of radiation modalities (i.e., electrons, X-rays, and proton), it will diversify treatments for diverse tumor types – including the deeply seated cases (26). The whole-thorax 18 Gy single dose FLASH (40 Gy/s) or Pulsed-FLASH RT resulted in a significantly smaller LLC than 18 Gy CONV RT. Immunofluorescence assay showed that the two FLASH groups seemed to recruit

CD3+, CD4+, and CD8+ cells better than CONV RT to the tumor microenvironment, possibly explaining why FLASH allows for better tumor growth control at isodoses. *The above details are the synopsis of a 2019 study by Rama et al. (23).*

Lastly, Kim et al. performed an *in vitro* study using Lewis lung carcinoma (LLC) to explore the effects of 16 MeV electron FLASH RT on the tumor microenvironment, specifically the extent of vascular collapse (27). Considering that FLASH RT protects normal tissues while damaging cancer cells, certain inherent differences between normal and cancer cells may be key in understanding the mechanisms of the FLASH effect.

A single dose of 15 Gy CONV RT activated myosin light chain (MLC), which is involved in cancer and endothelial cell membrane contraction that results in a reversible tumor vasculature collapse. It is understood that ROS activates MLC. However, 15 Gy FLASH RT did not cause tumor vascular collapse via MLC activation, even though its ROS production was higher than CONV. This puzzling result may be because this *in vitro* study was performed at 1 atm, where oxygen concentration is at 21% while cellular levels are much lower, ranging between 2 to 3%. For this reason, the FLASH effect may be better observed *in vivo*; *in vitro* investigation of the FLASH mechanism cannot achieve the oxygen concentration that is a critical part of the explanation for FLASH RT mechanisms of action – which will be discussed under the Mechanism section. Following irradiation, an increased number of myeloid cells had infiltrated the tumor, consistent with the observations made by Rama et al. While CONV RT relies on reoxygenation of the tumor and makes it vulnerable to subsequent RT sessions, the

tumor growth control mechanism by a single dose FLASH RT could be, at least in part, explained by the better preservation of the vasculature that allows the immune cells to invade the tumor microenvironment. *The above details are the synopsis of a 2020 study by Kim et al. (27).*

In conclusion, although electron beam is more commonly used in FLASH studies, HEX and proton therapies were also able to yield the FLASH effect and tumor growth control in murine lungs, which can broaden radiation modality options suitable for different cancer types. These studies have also provided possible dose parameter boundaries that may be appropriate for treating lung cancers.

2.2. Normal Skin

Radiotherapy involves penetrating the epithelium to reach the tumor site, making skin toxicity one of the main dose-limiting factors (28). We briefly saw that a 25 Gy FLASH RT in the lung did not induce skin damage while achieving tumor growth control (10). Since this 2014 study, a handful of research teams have evaluated the FLASH effect on murine, porcine, feline, canine, and human skin – the first FLASH RT clinical trial. Vozenin et al. explored the effects of 6 MeV electron FLASH RT on normal porcine skin (11). Single-dose treatments ranging from 22-34 Gy were administered to a mini pig at 300 Gy/s and 5 Gy/min dose rates. FLASH RT preserved hair follicles, while CONV RT permanently destroyed them even at six months post-IR. The spots irradiated by 28, 31, and 34 Gy CONV RT developed epithelial ulceration, dermal remodeling, and late skin fibro-necrosis associated with skin contraction that occurred ≥32 weeks post-treatment. The only adverse effect seen from FLASH RT was transient depilation three weeks after

28 and 31 Gy irradiations. FLASH irradiated skin was histologically no different from unirradiated skin. FLASH RT preserved CD34+ epidermal stem cells in the mini pig, a result consistent with the previous study that observed better lung progenitor cell protection by FLASH RT (7). The dose modifying factor of single dose FLASH was at least 20%. *The above details are the synopsis of a 2018 study by Vozenin et al. (11).*

A murine survival study by Soto et al. observed 16 MeV FLASH RT (180 Gy/s) doses at 10, 16, 20, and 30 Gy, and CONV RT (0.075 Gy/s) at 10, 16, and 20 Gy did not cause skin ulcerations at eight weeks post-IR (28). The skin toxicity scores between the treatment groups at 10 and 16 Gy doses were comparable. 16 Gy FLASH RT even reached a higher score than CONV RT – indicating a bit more skin damage – although the difference was not statistically significant. At 20 Gy, more CONV irradiated mice scored higher than FLASH mice. It was at 30 Gy when the noticeable sparing effect occurred where skin ulcerations were only observed from CONV irradiated mice. 100% of 30 Gy FLASH-irradiated animals survived while 60% survived after CONV RT. The difference was magnified at 40 Gy, where 80% of CONV mice scored the maximum value of 6 and had to be euthanized, while 40% of FLASH mice scored a 5, and only 20% were euthanized. 40 Gy FLASH RT survival rate was superior to that of 30 Gy CONV RT. *The above details are the synopsis of a 2020 study by Soto et al. (28).*

Velalopoulou et al. explored the FLASH effect using a proton beam on murine and canine skin (29). The average FLASH RT dose rate ranged from 69-124 Gy/s. 30 Gy FLASH RT on murine hind leg resulted in a median survival of >249 days and a 90%

survival rate compared to 50% CONV irradiated mice surviving in the median of 211 days. 45 Gy FLASH mice also had a better survival rate of 60% and median >256 days compared to 188 days with 30% survival by CONV RT. However, statistical significance could not be achieved due to the low count of surviving mice. Although radiation modalities and dose rates differed, the 30 Gy proton FLASH RT survival rate seemed consistent with the results from the previous 30 Gy electron FLASH RT study by Soto et al.

As it was observed from the molecular lung study by Fouillade et al., CONV irradiated mice had ten upregulated gene expression pathways, such as apoptotic and keratin signaling (differentiation and cornification), whose levels were normal in FLASH irradiated mice (7). On the other hand, FLASH RT upregulated tissue and vasculature repair pathways.

30 Gy CONV RT scored a significantly higher skin damage score than FLASH RT, which had reduced necrosis and hair follicle atrophy, consistent with the previous FLASH skin studies (11, 20). Lgr6+ hair follicle stem cell marker levels were significantly decreased in both FLASH and CONV groups, but FLASH RT provided slightly better preservation of the stem cells than CONV RT, which was still statistically significant. However, both 45 Gy FLASH and CONV irradiated mice reached the maximum skin damage score; although FLASH mice developed 10% more lymphedema than CONV irradiated mice, the overall severity was less. Further, 45 Gy FLASH mice had significantly less epidermal hyperplasia and less activation of myeloid cells, which is associated with inflammation due to radiation-induced damage. One of the markers of inflammation, TGFB1, was indeed elevated in the CONV group while indistinguishable

between FLASH and CTL mice. Similar TGFB1 results were observed in the canine skin after 8 and 12 Gy irradiation, where the difference was greater in the 12 Gy-treated cohort. A possible skin MTD at the dose rate of 69-124 Gy/s could be suggested where 45 Gy FLASH RT resulted in equivalent skin damage and incidence of lymphedema that was slightly more frequent than CONV, with lower severity. *The above details are the synopsis of a 2021 study by Velalopoulou et al. (29).*

TGFB1 is an early marker of skin damage that causes fibrosis in the lung and skin. 35 Gy FLASH proton pencil beam irradiation at 57 and 115 Gy/s reduced TGFB1 compared to 35 Gy CONV-RT administered at 1 Gy/s (30). FLASH irradiated groups had lower TGFB1 levels at 1-day post-IR than CONV irradiated animals, but higher than the control; the level returned to normal on the fourth day while remaining elevated in the CONV group. 100% of CONV irradiated mice scored the maximum skin toxicity of moist desquamation between 30- and 55-days post-IR, while 47% of 57 Gy/s FLASH irradiated mice developed maximum damage within 45 and 55 days. FLASH RT delayed the development of injury and attenuated toxicity. *The above details are the synopsis of a 2021 study by Cunningham et al. (30)*

Sørensen et al. also conducted a pencil beam scanning proton irradiation on murine skin, where the endpoints were early skin damage (11 to 25 days post-IR) and development of late fibrosis (31). The total doses administered ranged from 40 to 60 Gy. The average CONV RT dose rate was 0.38 Gy/s, and FLASH RT was 83 Gy/s. 99-100% of the CONV-irradiated mice across the dose groups suffered from acute toxicity

with a maximum score of 3.5. Only the mice irradiated with 60 Gy FLASH RT resulted in the same score at an equal frequency of 100%. All FLASH irradiated mice developed a skin condition score of 1.5, and TD50 (50% toxic dose-response) was reached at 54 Gy. *The above details are the synopsis of a 2022 study by Sørensen et al. (31).*

Zhang et al. explored the degrees of skin protection via proton FLASH RT dose escalation, coupled with oxygen tension factor. Among 130 Gy/s FLASH doses, 27 Gy reduced skin contraction to the greatest extent compared to 25 and 30 Gy under normoxia. At 75 days post-IR, only 25 Gy FLASH-irradiated animals had significantly less collagen deposition and epidermis thickening than the CONV RT counterpart, delivered at 0.4 Gy/s. No protective FLASH effect was observed in 30 Gy oxygen-breathing and 45 Gy hypoxic groups. Considering that the previous skin study by Velalopoulou et al. observed that 45 Gy FLASH and CONV RT resulted in similar skin damage, further studies should explore the effects of hypoxia with lower doses (29). *The above details are the synopsis of a 2023 study by Zhang et al. (32).*

Some of the limitations of the FLASH RT preclinical trials have been the heavy reliance on mouse models and uncertainties of long-term toxicity (33). The 2018 study with cat and mini pig reported no apparent toxicity at 6 months post-IR (11). In 2022, a randomized phase 3 clinical trial was performed with mini pigs and cat patients with spontaneous skin cancer to evaluate the effects of larger irradiation fields and long-term toxicities (33). Two out of the seven cats that received 30 Gy FLASH RT (1500 Gy/s) developed maximum grade bone necrosis at 12.5- and 15.1-months post-IR and one

Normal Skin Irradiation (Gy)	CONV RT	FLASH RT
8	Generally no difference in TGFB1 than CTL (29)	No difference in TGFB1 than CTL (29)
10	No ulceration 8 wk post-IR (28)	No ulceration 8 wk post-IR (28)
12	Strong increase in TGFB1 (29)	No difference in TGFB1 than CTL (29)
16	No ulceration 8 wk post-IR (28)	No ulceration 8 wk post-IR (28)
20	No ulceration 8 wk post-IR (28)	No ulceration 8 wk post-IR (28)
22	Depilation, hair regrowth (11)	Transient depilation, hair regrowth (11)
25	Depilation (11) Skin contraction, epidermal thickening and collagen deposition (32)	Transient depilation, hair regrowth (mini pig); acute erythema and moist desquamation that healed, depilation (cat) (11); 19.5% reduced contraction, reduced epidermis thickening and collagen deposition (32)
27	Skin contraction, epidermal thickening and collagen deposition (32)	Depilation (11); 26.5% reduced contraction; epidermal thickening and collagen deposition (32)
28	Ulceration, dermal remodeling, fibro-necrosis ≥32 wk post-IR (11)	Transient depilation (11)
30	Ulceration, 60% survival at 8 wk post-IR (28); severe necrosis, hair follicle atrophy, reduced stem cell, 50% survival (29); skin contraction, epidermal thickening and collagen deposition (32); no late bone necrosis (33)	No ulceration 8 wk post-IR, 100% survival by 180 Gy/s (28); reduced skin toxicity, better stem cell preservation, 90% survival 69-124 Gy/s (29); 10.2% reduced skin contraction; epidermal thickening and collagen deposition (32); late-term grade 3 bone necrosis (33)
31	Ulceration, dermal remodeling, fibro-necrosis ≥32 wk post-IR (11)	Transient depilation (11) Late toxicity with large irradiation field (33)
34	Ulceration, dermal remodeling, fibro-necrosis ≥32 wk post-IR (11)	Depilation (mini pig); moist desquamation that healed, depilation (cat) (11)
35	Elevated TGFB1 and 100% maximum toxicity (30)	Transiently elevated TGFB1 at day 1, back to normal at day 4, 47% maximum toxicity (30)
40	Maximum skin toxicity, 20% survival (28); 89% maximum skin toxicity (31)	High skin toxicity in 40% of the group, 80% survival (28); 0% maximum skin toxicity (31)
41	-	Acute erythema and moist desquamation that healed, depilation (11)
45	Maximum skin toxicity, 30% survival, greater TGFB1 (29); 83% maximum skin toxicity (31)	Maximum skin toxicity, 60% survival, no TGFB1 expression (29); 10% maximum skin toxicity (31)
51	100% maximum skin toxicity (31)	36.4% maximum skin toxicity (31)
60	100% maximum skin toxicity (31)	100% maximum skin toxicity (31)

Table 2. Comparisons of normal skin tissue responses after CONV and FLASH dose-rate irradiation by total dose

cat scored necrosis of the skin at 9.6 months and developed bone necrosis at 12.9 months. While these cats had been overdosed by up to 4.5-fold compared to CONV RT, none of the cats that received CONV RT developed osteoradionecrosis.

Enlarging the irradiation field to 3.5 x 4.5 and 8 x 8 cm compared to the 2.6 cm diameter from the 2018 study resulted in late cutaneous toxicity in mini pigs. Pigs developed permanent hyperkeratosis and skin contracture 6-8 months post IR, and severe telangiectasia at 5 months. Since these late toxicities were irradiation volume dependent, it would be of interest to perform future studies with FLASH microbeam therapy, which may reduce toxicities as seen previously in the lung study (22). Overall, this study addressed the important consideration for long-term toxicities. Studies should increase the follow-up period as the field continues the FLASH RT optimization effort. *The above details are the synopsis of a 2022 study by Rohrer Bley et al. (33).*

2.2.1. Skin cancer

A dose escalation study in cat patients with spontaneous squamous cell carcinoma showed moderate responses across tumor sizes and localizations (11). A 25 Gy dose induced transient acute stomatitis of the upper oral cavity; 27, 28, and 31 Gy did not indicate acute skin toxicity within the radiation field. 34 Gy induced acute and transient moist desquamation but soon recovered. 41 Gy was administered to the patient with a deeply seated tumor, which resulted in mucositis five weeks post-IR that eventually healed. At six months post-IR, 100% were tumor-free, but the 28 Gy-treated cat was euthanized at eight months post-IR due to recurrence, while the 31 Gy-treated patient had a recurrence managed via surgery at 21 months post-IR. At a median 18-month follow-up, the cat patients had permanent depilation within the radiation field but did not suffer from late toxicity and sustained their olfactory function.

The maximum tolerated dose was not achieved even at 41 Gy, but the dose escalation study stopped here as lower doses were sufficient to achieve complete tumor control. Compared to the 30 Gy FLASH in the murine lung, which resulted in adverse events at various dose rates, the skin tissues had better tolerability against higher doses. *For a more detailed review, refer to Vozenin et al. (11).*

Konradsson et al. performed a detailed dose escalation study in ten canine spontaneous skin cancer patients to explore the benefits of 10 MeV electron FLASH RT in treating pet cancer patients (29). 15, 20, 25, 30, and 35 Gy with an average dose rate of 400-500 Gy/s were administered within 30 to 75 ms. Although different types and locations of tumors did not allow for adequate comparisons, 11 out of 13 were met with some level of tumor growth control. Only the patient that received a 35 Gy FLASH RT developed a grade 3 skin adverse event (moist desquamation on nasal planum) at three months post-IR. Eight other patients scored 1, which is alopecia and mild dry desquamation. FLASH RT did not control malignant melanoma and oral basosquamous carcinoma in this study. *For a more detailed review, refer to Konradsson et al. (34).* Subcutaneously injected EMT6 breast cancer cell lines in mice revealed that 18 Gy HEX FLASH at 1000 Gy/s reasonably resulted in a significantly better tumor control than the lower 15 Gy dose of CONV RT at 0.01 Gy/s (21). However, the median survival was similar between FLASH (55 days) and CONV RT (59.5 days), while CTL was 35.5 days. *For a more detailed review, refer to Gao et al. (21).*

15 Gy CONV and 57 Gy/s FLASH proton pencil beam treatments were equally effective in the murine squamous cell carcinoma growth control compared to the control group. *For a more detailed review, refer to Cunningham et al. (30).*

C3H mouse mammary carcinoma were injected into the foot (31). Both proton CONV and FLASH RT did not result in recurrence at 90 days after irradiation, and the doses achieved 50% treatment were 49.1 and 51.1 Gy, respectively, which were not statistically different. *For a more detailed review, refer to Sørensen et al. (31).*

Tumor growth control was achieved in 16 cat cancer patients and remained tumor free during the follow up period. One 30 Gy FLASH-irradiated cat recurred at 371 days post-IR, and one CONV-irradiated cat at 644 days. Overall survival period did not differ significantly between treatment groups. *For a more detailed review, refer to Rohrer Bley et al. (33).*

The first FLASH RT clinical trial was performed with a 75-year-old patient with multi-resistant CD30+ T-cell cutaneous lymphoma on the skin surface (3.5 cm in diameter) (30). The patient had been treated with 110 CONV RT sessions but had developed resistance. In this clinical trial, a 15 Gy electron FLASH RT was administered within 90 ms and ten pulses. Six months of follow-up visits revealed a complete tumor response. There were no unexpected outcomes other than the interesting edema of the soft tissues that formed around the tumor, which was transient and never previously observed after CONV RT. The authors hypothesized that FLASH RT might interact with

the immune system differently than CONV RT, which is discussed later in section 1.4.1 (30). *For a more detailed review, refer to Bourhis et al. (35).*

2.3. **Normal Muscle and Bone**

Just like the skin, muscles and bone tissues are common organs affected during RT. However, the extent of the FLASH effect within these tissues have yet to be extensively investigated. Favaudon et al. briefly reported that the smooth muscles surrounding the bronchi and blood vessels were spared from radiation-induced apoptosis after 17 Gy electron FLASH RT (10).

Velalopoulou et al. examined canine and murine muscle and bone tissue responses of proton FLASH RT (29). 30 Gy proton FLASH RT (69-124 Gy/s) resulted in less muscle atrophy and bone resorption in the murine hind leg compared to CONV RT (28). RNA-seq analyses showed that CONV RT upregulated bone remodeling pathways and development of notochord and joint, while no change was observed after FLASH RT. This was the first indication that FLASH RT caused less bone damage. *For a more detailed review, refer to Velalopoulou et al. (29)*

Normal Muscle/Bone Irradiation (Gy)	**CONV RT**	**FLASH RT**
17	Radiation-induced apoptosis in smooth muscles (10)	No radiation-induced apoptosis in smooth muscles(10)
18	Damaged myofibril (36)	Myofibril structure protection (36)
30	Muscle atrophy and bone resorption (29)	Less muscle atrophy and bone resorption (29)
35	Greater leg contractures (30)	Significantly reduced leg contractures (30)

Table 3. Comparisons of normal muscle and bone tissue responses after CONV and FLASH dose-rate irradiation by total dose

Proton pencil beam FLASH RT study examined murine hind leg contracture over the 12 weeks after 35 Gy dose administration by CONV and 57 and 115 Gy/s FLASH RT (30).

There were no significant differences in contracture between the two dose rates of FLASH RT. Both FLASH irradiation induced significantly fewer leg contractures than CONV RT at 3-, 7-, and 12-weeks post-IR. *For a more detailed review, refer to Cunningham et al. (30)*

2.3.1. Sarcoma

So far, the FLASH effect has been observed across electron, X-ray, and proton radiation modalities. Tinganelli et al. explored the tumor treatment efficacy of a FLASH carbon ion, the first heavy ion FLASH RT using an osteosarcoma mouse model (36). LM8 cells that were injected in mice limb are known for metastasizing to the lungs. 18 Gy FLASH RT (100 Gy/s) significantly reduced lung metastasis compared to sham and CONV RT administered at 0.3 Gy/s. Tumor volumes in the limb were about 30% smaller in FLASH irradiated, which was statistically significant.

As for normal tissue protection, 18 Gy heavy ion FLASH RT (100 Gy/s) achieved better preservation of myofibril structure compared to CONV RT (0.3 Gy/s). This initial evidence for a FLASH effect via heavy ion irradiation allows possibilities to exploit the use of very heavy ions that treat hypoxic cancer cells. *The above details are the synopsis of a 2022 study by Tinganelli et al. (36).*

12 and 30 Gy proton FLASH and CONV RT showed equally effective tumor control capacities in two murine sarcoma models. *For a more detailed review, refer to Velalopoulou et al. (29)*

2.4. Normal Organs and Tissues of the Circulatory System

Connective tissues like the blood and its components are inevitable targets of radiotherapy. Previous studies of the lung and skin tissues have reported common immune responses of RT, such as lymphedema, which is major radiation-induced toxicity linked to chronic inflammation. Inflammation is associated with myeloid cell activation, such as neutrophils. CONV RT elevated a marker of inflammation TGFB1, while FLASH RT was indistinguishable from CTL in murine and canine skin (29).

In the first FLASH RT clinical trial, it was hypothesized that a single dose of UHDR radiation could result in fewer lymphocytes in the blood volume from being irradiated. Similarly, the immune cells infiltrating the tumor bed would not be destroyed by subsequent irradiation sessions, unlike during the multiple CONV RT sessions (35). This explanation may apply to the macrophage infiltration in the alveolar tissues after 30 Gy FLASH RT in murine lungs and better lymphocyte infiltration of the murine LLC microenvironment (10, 34).

Exploring the FLASH effect within the circulatory system has many important implications. First, one of the inevitable targets during radiotherapy is blood volume. Second, since FLASH RT experiments have focused on solid tumors, it is crucial to study its efficacy in controlling blood cancers and the outcomes of total-body irradiation (TBI) - including the effects on multipotent stem cell populations, such as those residing in the bone marrow. One of the mechanistic explanations for the FLASH effect could be that normal tissue protection is achieved via the protection of the multipotent stem cell populations from radiation-induced damage (26). A few studies have focused on

studying the differential immune responses between FLASH and CONV RT and tissues of the circulatory system.

One of the major injuries from TBI is radiation-induced aplasia, such as hematopoiesis inhibition (26). 6 MeV electron 4 Gy FLASH and CONV RT depressed immature human hematopoietic cell CD34+. However, mature CD45+ cells were present in 46% of FLASH-irradiated mice while they were eradicated entirely in all of the CONV mice at three months post-IR (n=17). This showed some stem cell protection by FLASH, while CONV RT was completely destructive.

In another experiment, CD34+ cells were matured into CD45+ cells before the introduction of M106 T-cell acute lymphoblastic leukemia (T-ALL) and consequent irradiation. 25% of FLASH and 100% CONV irradiated mice relapsed, and no hematopoiesis occurred in either cohort. FLASH RT resulted in a lower relapse rate than CONV RT, but it did not salvage normal hematopoiesis; therefore, the FLASH effect was not manifested.

While both FLASH and CONV RT at 4 Gy are toxic for normal human hematopoiesis, FLASH RT does preserve some human blood stem cells/progenitor cells better than CONV RT. The author speculates that their immunocompromised mouse model may yield different results than normal mice and that the low dosage administered may be the reason for the less pronounced FLASH effect. *The above details are the synopsis of 2020 study; for a more detailed review, refer to Chabi et al. (26).*

Lymphopenia is another common adverse effect of RT that involves decreased white blood cell counts, which affects treatment efficacy and patient survival (12).

Lymphocytes are highly radiosensitive and, like the skin, are one of the unintended targets of radiation. Since radiotherapy is frequently paired up with immunotherapy, it is integral to study the effects of FLASH RT on the immune system.

Venkatesulu et al. used 35 Gy/s UHDR RT to examine lymphocyte sparing in the murine heart and spleen because these organs are rich in lymphocytes and receive unintended radiation during esophageal or pancreatic cancer treatments (12). Circulating lymphocyte counts (CD3, CD4, CD8, CD19 cells) in female mice after a 10 Gy cardiac irradiation were depleted more by UHDR RT than CONV RT. At 24 days post-IR, only 50% of the cells irradiated with UHDR RT recovered, while 100% for CONV RT. A similar pattern was observed in male mice after a 5 Gy splenic RT, where UHDR depleted the cells significantly more than CONV RT.

This study illustrated the importance of defining FLASH RT beam parameters and refining tissue-specific dose rates because ≥40 Gy/s was derived from the murine lung study, not lymphocytes, which are more radiosensitive. This 35 Gy/s treatment is better referred to as UHDR rather than FLASH RT, as it is below the originally suggested ≥40 Gy/s FLASH dose rate by Favaudon et al. and may therefore be insufficient to yield a FLASH effect (10). More experiments should be conducted to determine proper FLASH dose rates for lymphocytes and explore the possibilities of reducing radiation-induced lymphopenia that reduces survival outcomes of RT-treated patients. *The above details are the synopsis of 2019 study; for a more detailed review, refer to Venkatesulu et al. (12).*

While damages to the blood and its components are systematic, injuries to the blood vessels specifically harm the organs in which they reside (37). Compromised vasculature integrity can be especially detrimental to organs like the brain because it may allow a slow buildup of toxins which can contribute to increased risks for stroke and other neurodegenerative diseases that decrease the quality of life. Yet, there has been only one study on the effects of FLASH RT on blood vessels thus far.

A single dose of 10 Gy whole-brain irradiation (WBI) via 6 MeV electron FLASH RT did not significantly alter blood vessel volumes at both early (24 hours) and late (1 month) time points post-IR (37). The instantaneous dose rate was 6.9 x 10^6 Gy/s. On the contrary, CONV RT (0.09 Gy/s) significantly increased the microvasculature volume and reduced tight junction proteins expression – indicating increased leakiness of the vessel.

25 Gy CONV RT similarly increased the vessel volume, while FLASH RT did not cause changes at one-week post-IR. Endothelial nitric oxide synthase (eNOS) activity was elevated after CONV RT in the hippocampus and astrocytes, while the tight junction protein occludin-5 expression was significantly reduced. Both factors indicated that CONV RT caused dilation and leakiness in the vessels. Although 25 Gy FLASH RT showed temporary microvasculature damage, eNOS and occludin-5 levels were similar to CTL. Furthermore, expression of another tight junction protein, claudin-5, was significantly increased in the hippocampus after FLASH RT, while CONV RT caused the opposite. These molecular studies provide a partial explanation of why the blood vessel volumes remained unchanged after FLASH RT and suggest that FLASH RT may be engaging in signaling pathways that are different from CONV RT. *The above details are*

the synopsis of a 2020 study; for a more detailed review, refer to Allen et al. (37).

12 types of cytokines were measured as systemic markers after 35 Gy PBS FLASH RT administered at 57 and 115 Gy/s dose rates (30). The difference in FLASH dose rates did not result in blood cytokine level differences. CONV RT (1 Gy/s) significantly decreased GM-CSF and G-CSF ratio compared to FLASH and CTL, indicating greater tissue toxicity. FLASH RT significantly increased interleukin 6 (IL-6) compared to both CTL and CONV groups. *For a more detailed review, refer to Cunningham et al. (30).*

High-energy X-ray is the most common modality, yet very few have applied it to FLASH RT studies. Zhu et al. conducted blood count analysis after 10 and 15 Gy high energy X-ray FLASH (>150 Gy/s) and CONV irradiation of mice intestines (38).
A complete blood count analysis at 24 hours after a 15 Gy dose showed greater immune cell counts (WBC, lymphocytes, and neutrophils) in both FLASH and CONV irradiated mice, but CONV RT resulted in a more significant increase. As for cytokines, TNF-alpha and IL-6 were also significantly elevated after both CONV and FLASH RT, but FLASH RT resulted in a greater increase. IL-10 was significantly depressed in both groups, but FLASH RT induced a greater decrease. Interestingly, this pattern reversed at 6 weeks after a 10 Gy dose. FLASH irradiated group had significantly lower WBC and lymphocytes compared to CTL and CONV, while CTL and CONV were not statistically different. TNF-a and IL-6 remained significantly elevated in the CONV group, but the FLASH group returned to levels comparable to CTL. IL-10 also remained significantly

depressed in CONV, but the FLASH group had significantly elevated compared to CTL and CONV.

Normal Systemic Irradiation (Gy)	CONV RT	FLASH RT
4	CD34+ depression, CD45+ 100% irradicated; no hematopoiesis (26)	CD34+ depression, CD45+ 54% irradicated, no hematopoiesis (26)
10	Increased vessel volume, decreased tight junction proteins (37); unaltered immune cell counts, elevated TNF-a, IL-6, depressed IL-10 6 wk post-IR (38)	Blood vessel volume and tight junction protein expression unaltered (37); depressed immune cell counts, no difference in TNF-a and IL-6 but elevated IL-10 compared to CTL 6 wk post-IR (38)
15	Increased immune cell counts, TNF-a, IL-6 1d post-IR, decreased IL-10 (38)	Increased immune cell counts, greater increase in TNF-a, IL-6 1d post-IR, greater decrease in IL-10 (38)
25	Increased vessel volume and NO synthase activity, decreased tight junction proteins (37)	Blood vessel unaltered 1 week post-IR, and NO synthase activity and occludin-5 similar to CTL, increased claudin-5 expression (37)
35	Decreased GM-CSF/G-CSF ratio, no changes in IL-6 (30)	Unaltered GM-CSF/G-CSF ratio, increased IL-6 (30)

Table 4. Comparisons of normal circulatory tissue responses after CONV and FLASH dose-rate irradiation by total dose

These data are consistent with previous FLASH RT studies speculating that FLASH RT allows quicker rebound to normal levels compared to CONV RT. However, since the doses of acute and late-term responses differed, it is premature to be conclusive. *For a more detailed review, refer to Zhu et al. (38).*

2.4.1. Cancerous organs & tissues of the Circulatory system

Chabi et al. explored the first FLASH TBI on three human T-ALL xenografts. In the first mouse model, M106 leukemic burden decreased 20 days post-IR for both FLASH and CONV RT (26). Although the difference was not statistically significant, FLASH-irradiated mice survived 6.5 days longer. In the second model with NSG immunodeficient mice, only FLASH RT decreased leukemic burden and significantly lengthened the lifespan. Two other human T-ALL xenografts, M108 and M114, revealed that FLASH RT was better at delaying the progression of M114, but only CONV TBI was

more effective at curing M108. The results indicated that the subtypes of T-ALL cells had different sensitivities to RT types for reasons yet to be elucidated. *For a more detailed review, refer to Chabi et al. (26).*

2.5. Normal Gut

Radiation-induced gastrointestinal toxicity is the dose-limiting factor in the treatment of abdominal/pelvic cancer, where 60 to 80% of patients suffer from fatigue, diarrhea, abdominal pain, nausea, delayed radiation enteropathy, etc. (39, 40). The gut is archetypally radiosensitive due to the crypt cells in the small intestines, and FLASH RT has shown reduced benefits compared to other organs like the skin and lungs. Although it is inappropriate to consider this dose rate as FLASH as previously discussed, a single 16 Gy electron UHDR RT (35 Gy/s) to the abdomen killed all mice within seven days, while the CONV RT group survived up to 15 days post-IR (12). Since the gut inevitably gets irradiated during treatments of other organs like the ovaries, it is essential to define appropriate FLASH dose parameters to maximize the FLASH effect in the gut (39). Whole-abdominal irradiation (WAI) of 15 Gy HEX FLASH RT (937 Gy/s) killed all cohorts within 4-5 days post-IR, while 60% of 12 Gy FLASH RT (700 Gy/s) irradiated mice survived the entirety of 150-day observation period post-IR (21). On the contrary, Levy et al. observed 90% survival by 16 Gy electron FLASH RT (216 Gy/s) for more than 90 days post-IR (40). Interestingly, the higher dose administered in lower dose rate by Levy et al. allowed better survivability than 12 and 15 Gy HEX FLASH RT. None of the 12, 15, and 16 Gy CONV irradiated mice survived.

Early responding tissues like the gut are more sensitive to dose rate than the total dose. So, rather than radiation modalities, the lower dose rate used by Levy et al. compared

to that by Gao et al. might explain the differences in survival among the aforementioned studies. A proof-of-concept proton FLASH RT study by Zhang et al. also aligns with this possible explanation. 100% of 13 & 16 Gy proton FLASH irradiated mice survived through the 21 days of observation period; the average dose rate was 120 Gy/s, lower than that of the previous two studies (25). However, 19 and 22 Gy FLASH RT resulted in deaths around the same time as CONV irradiated mice at the same doses, indicating that the FLASH effect was abolished, and that the abdominal FLASH RT dose should remain below at least 19 Gy. Loo et al. did not specify survival rates for each dosage in their short poster abstract, but 90% of 13-19 Gy electron FLASH WAI resulted in 90% survival at 210 Gy/s (41). It would be interesting to see where single-dose FLASH RT would fit in this pattern since it has orders of magnitude greater dose rates. Also, more experiments should determine the appropriate dose rate for maximized protection as LD50 was higher at 210 Gy/s than 70 Gy/s, and it is apparent that not all lower dose rates are better for the gut (41).

16 Gy FLASH and CONV irradiated groups induced mucosal damage. Still, FLASH-irradiated mice had a two-times greater number of regenerating crypts than CONV IR and no histological difference compared to the CTL (40). Further, a sublethal dose of 14 Gy decreased the number of stool pellets in both groups, but FLASH-irradiated mice recovered faster and had better intestinal epithelium integrity. Both 12 and 14 Gy FLASH IR groups had superior regeneration of crypts compared to CONV RT at the same doses.

FLASH irradiation is not without damage but allows for better recovery and reduced cell apoptosis, as indicated via TUNEL assay and cleaved caspase-3 staining (40). FLASH

RT also did not deplete leucine-rich G-protein coupled receptors (Lgr5) to the same extent as CONV RT. Lgr5 is expressed continuously in crypt cells and is depleted by high radiation doses. The remaining challenges before FLASH RT translate to clinical trials are limited target volumes appropriate for FLASH irradiation and whether a fractionation regimen could yield a FLASH effect in the gut (40). *The above details are the synopsis of a 2020 study; for a more detailed review, refer to Levy et al. (40).*

Zhang et al. also observed late intestinal effects where both 16 Gy CONV and FLASH RT (120 Gy/s) resulted in collagen deposition, hyperplastic submucosa and muscularis, and infiltration of inflammatory cells (25). FLASH RT group seemed to have an improved repair mechanism but could not be compared statistically as only two CONV irradiated mice survived. *For a more detailed review, refer to Zhang et al. (25).*

Diffenderfer et al. performed the first proton FLASH RT where 15 Gy WAI was used to study the acute effect at 3.5 days post-IR and 18 Gy for a long-term effect eight weeks post-IR (24). The dose rate ranged between 70 and 88 Gy/s. EdU+ measurement showed that 15 Gy FLASH RT resulted in more regenerating crypt cells than CONV irradiated mice, just as Levy et al. observed. However, both were significantly decreased compared to the CTL group. For the long-term effect at eight weeks post-IR, Masson's trichrome staining showed that 18 Gy FLASH RT resulted in reduced fibrosis compared to CONV RT, and it was comparable to the CTL group. As previously stated, FLASH RT is not without damage, but the difference in outcomes lies in its superior

preservation of repair capacity. *For a more detailed review, refer to Diffenderfer et al. (24).*

During a FLASH RT ovarian cancer study, more regenerating crypts in the jejunum were observed after 14 Gy electron FLASH (210 Gy/s) than CONV RT, consistent with all FLASH RT studies of the gut (42). *For a more detailed review, refer to Eggold et al. (42).*

Proton RT involves a unique dose delivery mechanism where the highest LET occurs within the Bragg peak region, and dose deposition is reduced at the entrance point. Kim et al. were the first to investigate the effect of the FLASH dose rate at the Bragg peak (43). WAI 15 Gy proton FLASH RT (96-120 Gy/s) resulted in more regenerating crypt cells than CONV RT at the Bragg peak, but both levels were significantly depressed compared to CTL. Since the entrance dose for FLASH and CONV RT did not result in differences, future proton FLASH RT studies can focus on investigating the effects within the Bragg peak region (43). *For a more detailed review, refer to Kim et al. (43).*

The study by Ruan et al. was the first to explore the microbial profiles after WAI electron FLASH RT (39). Dose escalation ranged from 7.5 to 20 Gy, and dose rates between 2.2 to 5.9 x 106 Gy/s. Crypt survival was normalized to the number of cells per crypt in CTL mice, where 7.5, 10, and 12.5 Gy FLASH RT resulted in better survival in 9-10 weeks old mice, while only the 12.5 Gy dose yielded significant results in 30-31 weeks old

mice. 90% crypt depletion occurred at 12.7 Gy CONV RT and 13.9 Gy FLASH RT. The dose-modifying factor for both age groups was 1.1.

Ruan et al. further investigated the effects of temporal pulse structure on crypt survival, where 11.2 Gy WAI via various pulses were observed. 11.2 Gy delivered within 0.04 seconds resulted in better crypt survival by five pulses rather than two – each pulse had a dose rate of 56 Gy/s as opposed to 140 Gy/s. When the delivery time is kept the same, increasing the number of pulses was beneficial to 9-10 weeks-old mice because it followed the notion that lower dose rates may enhance protection. Interestingly, the opposite was observed in 30-31 weeks-old mice when 12.5 Gy was delivered within the same delivery time and pulses where two pulses resulted in greater survival. As previously stated, the older mice also required a higher dose of 12.5 Gy to secure improved crypt survival than younger mice. These results suggest that the age factor should be accounted for when finding FLASH dose parameters.

In this study, an increased number of pulses while increasing delivery time resulted in a significantly decreased crypt survival. Yet, increasing the number of pulses while keeping the delivery time constant (thus, decreasing both dose and dose rate per pulse), resulted in better crypt survival (39). Therefore, delivery time, rather than the number of pulses, may be more responsible for determining whether we can yield a FLASH effect. Regarding the dose rate being a critical factor for gut protection, a single pulse resulted in the best crypt survival via Swiss roll-based crypt assay, similar to what Loo et al. observed (41).

Lastly, the gut microbiome was analyzed via 16S rRNA, where both CONV and FLASH RT decreased overall species diversity and evenness. CONV RT also reduced species

richness and certain strains, such as Clostridia (39). Bacilli class increased after CONV RT, which has been associated with radiation-induced diarrhea. Microbial functions such as bacterial invasion, bile secretion, and arachidonic acid metabolism in CONV-irradiated mice were also altered. Based on these results, gut microbes are likely to be more sensitive, and CONV easily dysregulates their activities than FLASH RT. Considering that radiation-induced changes in the gut microbiome are directly related to intestinal injury, the reduced changes exerted may partially explain the reduced gut injury by FLASH RT. *For a more detailed review, refer to Ruan et al. (39).*

An acute LD50 study was conducted with 50 mice using a proton beam. 30 mice were irradiated with 10 – 19 Gy FLASH RT at 100 Gy/s, and 20 mice were irradiated with 10 – 16 Gy CONV RT (0.1 Gy/s) in the abdomen. The LD50 for CONV and FLASH RT were 13.5 and 14.1 Gy, respectively. FLASH RT resulted in a maximum of 19% better survivability than CONV RT. *For a more detailed review, refer to Evans et al. (44).*

15 Gy high-energy X-ray abdominal irradiation did not result in statistical differences in survival at 6 weeks after FLASH or CONV RT, where 7/8 and 5/8 survived, respectively (38). However, FLASH irradiated mice regained body weight faster and had significantly less acute damage, as none developed grade 3 intestinal toxicity. IHC results showed reduced neutrophils and macrophages in both groups compared to CTL, but the number of crypts was unaltered by FLASH RT while significantly depressed in the CONV group. Interestingly, ROS generation was marginally greater after FLASH RT ($p=0.055$), but lipid peroxidation was better controlled compared to the CONV group ($p=0.015$).

For a more detailed review, refer to Zhu et al. (38).

Normal Gut Irradiation (Gy)	CONV RT	FLASH RT
7.5	Poor crypt survival in juvenile mice (39)	Better crypt survival in juvenile mice (39)
10	Poor crypt survival in juvenile mice (39)	Better crypt survival in juvenile mice (39)
12	100% died (21); depressed crypt regeneration (40)	60% survival at 150 d post-IR (21); superior crypt regeneration (40)
12.5	90% crypt depletion, microbiome richness and species diversity decreased (39)	Better crypt survival in juvenile and old mice, maintained microbiome richness, diversity declined (39)
13	-	100% survival 21 d post-IR (120 Gy/s) (25)
13.5	LD50 (44)	-
14	Depressed crypt regeneration (40, 42, 43)	Superior crypt regeneration (40, 42, 43); 90% crypt depletion (39); LD50 (44)
15	100% died (21); depressed crypt regeneration at 3.5 d and 6 wk post-IR (24, 38 respectively); more lipid peroxidation (38)	100% died 5 d post-IR (937 Gy/s) (21); superior crypt regeneration at 3.5 d and 6 wk post-IR(24, 38 respectively); less lipid peroxidation (38)
16	100% died; mucosal damage, depressed crypt regeneration (40); collagen deposition, immune cell infiltration (25)	90% survival 90 d post-IR (216 Gy/s), less mucosal damage, 2x crypt regeneration (40); 100% survival 21 d post-IR (120 Gy/s), collagen deposition, immune cell infiltration (25)
18	Fibrosis at 8 wk post-IR (24)	Reduced fibrosis at 8 wk post-IR (24)
19	-	100% died 12 d post-IR (120 Gy/s) (25)
22	-	100% died 10 d post-IR (120 Gy/s) (25)

Table 5. Comparisons of normal intestinal tissue responses after CONV and FLASH dose-rate irradiation by total dose

2.5.1. Gut Cancer

MH641905 pancreatic tumor cells were injected into the flanks and received a single 18 Gy FLASH and CONV RT. Both treatment groups showed comparable tumor control at the entrance and the Bragg peak. 85% of the FLASH irradiated mice survived, while 70% of CONV irradiated mice died within 20 days post-IR. *For more details, refer to Kim et al. (43).*

Another MH641905 pancreatic flank tumor study observed statistically similar tumor volume reduction by 12 and 18 Gy FLASH or CONV proton RT. *For more details, refer to Diffenderfer et al. (24).*

2.6. Ovary

There is not yet a study that has looked at the effects of FLASH WAI on normal ovarian functions.

2.6.1. Ovarian Cancer

Ovarian cancer is one of the deadliest malignancies, with 70-80% recurrence rates and a 5-year survival rate below 50% (45, 46). One of the reasons for poor prognosis is that most patients are at the advanced stage at the time of diagnosis. Checkpoint inhibition is a promising immunotherapy, but advanced ovarian cancer is often resistant or relapses to this therapy alone. Since radiotherapy is commonly combined with immunotherapy to treat cancer, it is crucial to evaluate the outcomes of novel FLASH RT when used with immunotherapy (42). Some immunologic reactions after FLASH RT have been documented, such as increased immune cell infiltration (10, 23, 27). This has exciting implications for enhanced treatment potentials by FLASH RT as T-cell infiltration into the tumor microenvironment has correlated with better survival and immunotherapeutic response (42).

Eggold et al. irradiated ID8 or UPK10 ovarian cell lines injected intraperitoneally via CONV (0.126 Gy/s) and FLASH RT (210 Gy/s). The study aimed to investigate the immunomodulatory effects of FLASH RT with anti-programmed cell death-1 (aPD-1) checkpoint blockage (42). 14 Gy FLASH and CONV RT caused a similar decline in ovarian tumor cell count and weight at 27 days post-IR. At the early time point of 4 days

post-IR, both treatments had reduced CD45+ leukocytes, T cells, and B cells in the tumor microenvironment compared to the CTL group. The FLASH irradiated tumor had more CD4+ cells than CONV irradiated tumors. At 17 days post-IR, CONV and FLASH RT increased cytolytic CD8+ T cells compared to CTL. This indicated that FLASH RT could induce the same immune response as CONV RT – by decreasing regulatory T cells and increasing cytolytic CD8+ T cells in the tumor microenvironment. FLASH RT combined with aPD-1 treatment enhanced the infiltration of CD8+ in both ID-8 and UPK10 ovarian cancer models.

UPK10 model showed similar tumor growth control between treatment groups: aPD-1, 14 Gy CONV RT,14 Gy FLASH RT, CONV RT + aPD1, FLASH + aPD1, and CTL. However, only the combined therapies increased CD8+ T cell infiltration compared to CTL, indicating a better prognosis. FLASH RT + aPD-1 achieved similar immunomodulation as CONV + aPD1 but with significantly reduced gastrointestinal toxicity. Mice treated with FLASH RT and immunotherapy recovered body weight, stool pellets, and blood sample levels to normal levels within 17 days. *The above details are the synopsis of a 2021 study; for a more detailed review, refer to Eggold et al. (42).*

ID8 ovarian cancer peritoneal metastasis mice model was subject to 14 Gy FLASH and CONV RT (40). CONV-irradiated mice produced less stool at day five post-IR and had 5% more weight loss than the FLASH IR group on day 6. Both treatments similarly reduced the tumor cell counts. *For a more detailed review, refer to Levy et al. (40).*

2.7. Normal Brain

The brain is a highly fatty organ that shows delayed responses to irradiation (47). 50-90% of adult brain cancer patients commonly suffer from a slow progression of irreversible cognitive decline over the years following radiotherapy (48). The inability to prevent patients from neurocognitive complications like learning, memory and attention deficits, mood disorders, cerebral microbleeds, and increased risk of stroke compromises the quality of life in surviving patients (49-53). Preventing neuroinflammation may help reduce progressive cognitive decline (47). FLASH RT may be involved in this pathway as a few *in vivo* experiments across the organ systems have observed reduced inflammatory markers after FLASH RT (7,10, 29). Within the FLASH RT brain studies, similar inflammatory pathway attenuations have been observed (57, 58, 62).

Montay-Gruel et al. 2017 performed the first FLASH RT study that observed the sparing of cognitive functions in the murine brain (54). The authors hypothesized that the FLASH effect is related to the extremely short exposure time and experimented with various dose rates to precisely identify the dose parameters that yield the FLASH effect in the brain. The dose rates in this study ranged from the CONV dose rate of 0.1 through 500 Gy/s, delivering a 10 Gy whole brain irradiation (WBI). Radiation-induced brain toxicity is partially due to altered hippocampal neurogenesis, where the earliest manifestation in mice is one month after a single 10 Gy dose (55).

At two months post-IR, CONV-irradiated mice performed poorly on Novel Object Recognition tests (NOR). At the same time, single pulse (delivered within 1.8 us), 500 Gy/s, and 100 Gy/s FLASH irradiated groups showed no difference compared to the

CTL group. This cognition preservation started to decline with the decreasing dose rate – 60 and 30 Gy/s – where the decline in performance was stark. The FLASH effect was lost below 30 Gy/s. Memory was completely impaired in 10 Gy CONV irradiated mice, as expected. Even though a single 10 Gy dose commonly results in a late cognitive deficit, mice irradiated at a FLASH dose rate above 30 Gy/s showed the opposite results (37).

Lastly, at the cellular level, BdrU analysis showed hippocampal neurogenesis was depressed in both FLASH and CONV irradiated groups compared to CTL but more severely by CONV RT. The FLASH effect in the brain may partially rely on neural stem cell preservation. *The above details are the synopsis of a 2017 study; for a more detailed review, refer to Montay-Gruel et al. (54).*

In 2018, Montay-Gruel et al. explored the possibilities of inducing the FLASH effect in the brain with broad-beam X-rays (20). 10 Gy FLASH whole-brain irradiation at a mean dose rate of 37 Gy/s spared cognition at both 2- and 6-months post-IR, while CONV irradiated group performed poorly at both time points. Similarly to their 2017 study, both treatments significantly depleted cell divisions in the hippocampus compared to the untreated CTL, but CONV RT caused significantly more depletion than FLASH RT. FLASH RT spared astrogliosis response at the cellular level, while the level was significantly elevated in the conventionally irradiated group. The normal tissue-sparing effect by X-ray FLASH RT was comparable to the results from the 2017 electron FLASH study performed by the same group. *The above details are the synopsis of a 2018 study; for a more detailed review, refer to Montay-Gruel et al. (20).*

Following their 2017 *in vivo* FLASH RT brain study, Montay-Gruel et al. expanded on the types of behavioral tests. They documented the long-term cognitive effects six months after electron CONV and FLASH RT (56). Per NOR test results, 10 and 12 Gy FLASH irradiations (>100 Gy/s) spared cognition one-month post-IR. However, the FLASH effect was lost when the total dosage was increased to 14 Gy.

10 Gy FLASH irradiated mice showed no statistical difference from CTL mice and reduced anxiety or depression-like behavior at six months post-IR compared to the CONV group. Minimizing mood disorder-like symptoms indicated that FLASH RT does not trigger neurotoxic pathways. The authors speculated that this might be because FLASH RT minimizes reactive oxygen species production (56). Reduced oxidative stress leads to testable biological manifestations such as astrogliosis, where glial fibrillary acidic protein (GFAP) expression serves as an astrocyte marker for immunoreactivity against damages like the destruction of neurons and infection.

10 Gy CONV RT increased GFAP expression at 14 days and 2 months post-IR. In contrast, 10 Gy FLASH RT resulted in comparable GFAP levels with the unirradiated CTL group at later time points. This beneficial FLASH effect being sustained until the late time points has exciting implications for radiotherapeutic treatment of the late-responding brain. Further analysis of microglial activation at one- and six-month post-IR showed similar results where CONV RT caused elevation at both time points. At the same time, FLASH RT was statistically indistinguishable from the CTL group.

Irradiation is known to cause structural plasticity in the brain, but FLASH RT surprisingly did not elicit such a response. Morphological differences between CONV and FLASH irradiated brains included reduced dendritic spine count and complexity in CONV-

irradiated mice six months post-IR. These results showed that FLASH RT does not induce the typical radiation-driven responses seen in the brains at early or late time points, indicating better treatment outcome possibilities in brain cancer surviving patients once it successfully translates clinically. *The above details are the synopsis of a 2019 study; for a more detailed review, refer to Montay-Gruel et al. (56).*

Simmons et al. explored radiation-induced damages as indicated by memory loss through NOR test and hippocampal dendritic spine density, microglial activation, and proinflammatory cytokine activation ten weeks post-IR (57). 30 Gy electron FLASH RT (250 Gy/s) spared memory functions and dendritic spine density, while 30 Gy CONV RT (0.13 Gy/s) significantly reduced NOR performance. Microglial activation after FLASH RT was in between CTL and CONV RT levels, where the latter showed a significant increase in this inflammatory response. Lastly, among the ten surveyed cytokines expressed by microglia, 5 were significantly elevated after CONV RT, while 3 (TNFa, IL-1b, and KC/GRO) were by FLASH RT. *The above details are the synopsis of a 2019 study; for a more detailed review, refer to Simmons et al. (57).*

Previous studies have shown that the downstream cognitive outcomes are more attenuated by FLASH RT (54, 56). Since FLASH RT did not induce microglial activation, which is the brain's immune response, Montay-Gruel et al. 2020 performed a further investigation of astrogliosis in conjunction with the immune complement system activation in the murine brain after FLASH RT (56, 58). 10 Gy FLASH RT delivered in 1.8 us did not cause hypertrophy in hippocampal astrocytes. At the same time, CONV

RT significantly changed the morphology and increased GFAP expression at one-month post-IR (58).

Next, immune complement system proteins were assayed. C1q is involved with microglia that play a role in neurodegenerative conditions. Overall, C1q complement protein expression was significantly increased after both CONV and FLASH RT, but the latter induced greater levels throughout the brain. However, the colocalization of C1q with activated microglial surface revealed that CONV RT significantly elevated the expression, while FLASH RT did not. Astrocytes also express C1q when undergoing neurological pathologies. There was a significant increase in colocalized GFAP and C1q after both CONV and FLASH RT.

Pro-inflammatory C3 anaphylatoxin expression by astrocytes also showed that CONV and FLASH RT significantly elevated expressions at one-month post-IR, even though FLASH RT did not induce astrogliosis. Lastly, TLR4 expression was measured as C3 interacts with TLR4 to induce inflammation. CONV RT significantly increased TLR4 expression on the surface of reactive astrocytes, but the levels after FLASH RT were comparable to the unirradiated control. The attenuated inflammatory responses after FLASH RT may explain the better cognitive preservation seen in our animal models.

The above details are the synopsis of a 2020 study; for a more detailed review, refer to Montay-Gruel et al. (58).

About 500 new cases of medulloblastoma are diagnosed annually in the US, with 15-20% occurring in patients under two years of age (59, 60). Although these pediatric patients have a high survival rate exceeding 80%, cognitive decline over the years

following treatment ruins the quality of life (59-61). Radiation therapy is critical yet complicated in this patient population because developing CNS is highly sensitive to radiation.

As previously seen in the study by Ruan et al., FLASH RT induced different responses in the gut by the age factor (39). Here, the authors performed a proof-of-principle analysis with juvenile mice by administrating a single 8 Gy WBI Gy/s, considering immature brains are more susceptible to radiation-induced toxicity (53).

Five behavior tests were performed to examine various aspects of murine innate behavior. Objects in Updated Location test (OUL) is designed to explore the rodent's preference for novelty. CONV irradiated group performed poorly at two- and four-months post-IR, while FLASH mice did poorly at two months but recovered by four months post-IR. This again shows that FLASH RT is not damage-free but better preserves recovery potentials than CONV RT. At four months post-IR, NOR, light-dark box (LDB), and social interaction test (SIT) were performed where FLASH animals had comparable results as the CTL for NOR and SIT while CONV irradiated mice performed poorly. LDB test that evaluates mood disorder showed that FLASH irradiated mice showed greater light-dark transitions compared to CONV and CTL groups. However, the total time spent under the light did not differ across the groups. Lastly, a fear extinction memory test showed that FLASH mice were able to forgo their learned fear response to a stimulus once the stimulus was removed. In contrast, CONV-irradiated mice continuously showed increased freezing behaviors and could not unlearn the behavior even after the trigger was removed.

Since juvenile mice brains have more neural stem and progenitor cells, a greater sparing of these cells would result in favorable cognitive outcomes. The molecular levels of doublecortin positive cells, BrdU+, and NeuN after FLASH RT were similar to that of the CTL while significantly depressed by CONV RT. As Montay-Gruel et al. 2019 showed, activated microglia levels were higher in CONV-irradiated mice than in FLASH. Lastly, the effects of FLASH RT on the endocrine system revealed that FLASH RT preserved the plasma growth hormone levels comparable to CTL, while CONV RT significantly reduced it by two folds. Growth hormones in juvenile mice are critical for normal development, and FLASH RT seemed to have superior protection of the hypothalamic-pituitary axis (4).

The FLASH effect in the brain, comprised of salvaging the cognitive functions, neural stem cell counts, and hormonal functions, is critical in preserving neuronal health in child patients, posing the exciting potential for FLASH RT in clinics. *The above details are the synopsis of a 2020 study; for a more detailed review, refer to Alaghband et al. (53).*

Dokic et al. performed the only proton FLASH brain irradiation thus far. They reported the levels of DNA DSB, brain microvascular density and structural integrity, and inflammatory response via activated microglia (62). At one week post-IR, 10 Gy FLASH RT (120 Gy/s) was found to have induced 2.5-fold less yH2AX positive cells compared to CONV RT (0.17 Gy/s) at the Bragg peak region. It is unclear whether there were any differences between FLASH and unirradiated CTL groups. CD31+ marker of vascular density was significantly reduced in the CONV irradiated group compared to the CTL and FLASH groups. Closer analyses showed long and medium-sized vessels differed

between CONV and FLASH-IR groups. Lastly, proton FLASH RT did not induce microglial activation, while CONV RT significantly increased this neuroinflammatory response. *The above details are the synopsis of a 2022 study; for a more detailed review, refer to Dokic et al. (62).*

Normal Brain Irradiation (Gy)	CONV RT	FLASH RT
8	Poor behavioral outcomes 2 and 4 mo post-IR in juvenile mice, depleted neural stem cells and plasma growth hormones, elevated microglial activation (53)	Poor behavioral outcomes 2 mo but recovered by 4 mo post-IR, preservation of neural stem cells and plasma growth hormone, slightly elevated activated microglia (53)
10	Cognition and hippocampal neurogenesis significantly decreased at 2 mo post-IR (20, 55); astrogliosis (20, 58); cognitive decline, mood-disorder 1 mo post-IR, astrogliosis at 0.5 and 2 mo post-IR (56); astrocyte hypertrophy, significantly increased GFAP+Cq1. C3, and TLR4 expression (58); significantly more DNA DSB at 1 wk post-IR, reduced vascular density, microglial activation (62)	Cognition comparable to CTL at >60 Gy/s, hippocampal neurogenesis significantly decreased but better than CONV RT at 2 mo post-IR (20, 55); no astrogliosis (20, 56); cognition and mood-disorder spared 1 mo post-IR, no astrogliosis (56); no astrocyte hypertrophy, significantly increased GFAP+Cq1 and C3 expression, no difference in inflammatory TLR4 (58); less DNA DSB at 1 wk post-IR, less reduction in vascular density, no microglial activation (62)
12	Cognitive decline 1 mo post-IR (56)	Cognition spared 1 mo post-IR (56)
14	-	Cognition not spared (56)
25	Neural cell apoptosis (37)	Less neural cell apoptosis than CONV but elevated Tdt+ than CTL (37)
30	Memory and hippocampal dendritic spine density loss, elevated microglial activation, 5/10 elevated cytokine expressions (57)	Memory and hippocampal dendritic spine density preservation, slight elevation of microglial activation, 3/10 elevated cytokine expressions (57)

Table 6. Comparisons of normal brain tissue responses after CONV and FLASH dose-rate irradiation by total dose

Along with the protective effects of FLASH RT on the BBB, Allen et al. explored the effects of a single 25 Gy dose on inducing neural cell apoptosis in the subventricular zone and dentate gyrus – the sites of active neurogenesis (37). FLASH RT induced less apoptosis within these regions than CONV RT, although Tdt+ cells were still elevated compared to CTL. *For a more detailed review, refer to Allen et al. (37).*

2.7.1 Brain Cancer

The fractionated regimen is the standard treatment for radioresistant glioblastoma (63). Considering that the FLASH effect is suggested by reduced ROS production, which might implicate reduced tumoricidal efficacy, it was important to document the outcomes of glioblastoma treatment via fractionated FLASH RT. Murine H454 glioblastoma cells were implanted in nude mice. After 3 days, the animals were treated with treatment regimens: single 10 Gy, single 14 Gy, daily doses of 4 x 3.5 Gy, 2 x 7 Gy, and 3 x 10 Gy. There was a hemibrain 25 Gy single dose irradiation. The instantaneous dose rate was >1.8x10^6 Gy/s.

At 4 weeks post-IR, single doses of 10 and 14 Gy FLASH and CONV RT achieved comparable tumor growth control compared to CTL but did not reach full growth control. As seen in previous studies, the 10 Gy FLASH-irradiated group showed comparable cognitive functions compared to CTL, while CONV RT significantly reduced performance (20, 55, 56, 63). Moreover, 14 Gy FLASH RT reduced cognitive sparing, as seen previously (56, 63). Therefore, this dose was fractionated and delivered in two pulses – 2 x 7 Gy doses. This fractionated regimen resulted in cognitive sparing comparable to the CTL group but did not change the overall survivability of animals or tumor growth control efficacy compared to the single 14 Gy. Next, the effect of 4 x 3.5 Gy was explored as this resembles a clinical dose fractionation. CONV and FLASH RT resulted in limited tumor growth delay and similar survivability, but FLASH RT did not spare cognition compared to CONV RT.

As none of the abovementioned regimens reached effective tumor growth control, a 3 x 10 Gy hypo-fractionated regimen was explored. 60 Gy was delivered in 2 days, spaced

by 48 hours. CONV and FLASH RT showed comparable tumor control and improved survival compared to the previous regimens. FLASH RT preserved cognition comparable to the CTL, while CONV RT resulted in a significant decrease in memory compared to CTL and FLASH RT.

Lastly, 25 Gy irradiation of the tumor-bearing hemibrain significantly improved tumor control and survivability. However, cognition was not spared, as seen previously by WBI. *The above details are the synopsis of a 2021 study; for a more detailed review, refer to Montay-Gruel et al. (63).*

In vivo Study types	Number of studies	Reference
Clinical Trial	1	35
Murine (mouse)	26	7, 10, 20, 21, 24, 25, 26, 28, 29, 30, 31, 32, 37, 38, 39, 40, 41, 42, 43, 44, 53, 54, 56, 57, 58, 62
Murine (rat)	1	22
Canine	2	29, 34
Feline	2	11, 33
Porcine	2	11, 33
Human	1	35
Electron FLASH	21	7, 10, 11, 26, 27, 28, 29, 33, 34, 35, 36, 37, 39, 40, 41, 42, 53, 54, 56, 57, 58
Photon FLASH	4	20, 21, 22, 38
Proton FLASH	10	23, 24, 25, 29, 30, 31, 32, 43, 44, 62
Heavy ion FLASH	1	36
Normal tissue	25	7, 10, 11, 20, 21, 24, 25, 26, 28, 29, 30, 32, 33, 37, 38, 39, 40, 41, 42, 43, 44, 53, 54, 56, 57, 58, 62, 63
Malignant cells/tissue	17	10, 11, 21, 23, 24, 26, 27, 29, 30, 31, 33, 34, 35, 36, 40, 42, 43, 63, 64
Normal Lung	4	7, 10, 21, 22
Normal Skin	7	11, 28, 29, 30, 31, 32, 33
Normal Muscle and Bone	3	10, 29, 30
Normal Circulatory/Immune system	3	26, 30, 37
Normal Gut	10	21, 24, 25, 38, 39, 40, 41, 42, 43, 44
Normal Ovary	0	None – only ovarian cancer studies
Normal Brain	8	20, 37, 53, 54, 56, 57, 58, 62

Table 7. Published FLASH RT studies organized by category

Tissue	Species	Tumor Type	Rad. Modality	Total Dose(s) (Gy)	Mean Dose Rate (Gy/s)	Reference
Lung	Murine	Orthotopic, isogenic TC-1 (mouse lung carcinoma	Electron (4.5 MeV)	15, 23, 28	≥40	10
	Murine	Orthotopic, isogenic Lewis Lung Carcinoma	Proton (0.5 nA)	18	40	23
	Murine	Isogenic xenograft Lewis Lung Carcinoma	Electron (16 MeV)	15	352.1 ± 4.0	27
Skin	Feline	Spontaneous squamous cell carcinoma	Electron (4.5 & 6 MeV)	25, 27, 28, 31, 34, 41	300	11
	Murine	Orthotopic, isogenic MOC1 and MOC2	Proton (250 MeV)	15	57, 115	30
	Feline	Spontaneous squamous cell carcinoma	Electron (6 MeV)	48	1500	33
	Canine	Spontaneous superficial solid tumors (carcinoma, sarcoma, mast cell, melanoma)	Electron (10 MeV)	15, 20, 25, 30, 35	430 – 500	34
Muscle/Bone	Murine	Isogenic, orthotopic subcutaneous fibrosarcoma	Proton (230 MeV)	12, 30	69 - 124	29
	Canine	Spontaneous osteosarcoma	Proton (230 MeV)	4, 8, 12	102.59	29
	Murine	Isogenic, orthotopic mouse osteosarcoma LM8	Heavy ion ^{12}C (240 MeV/n)	18	100	36
Blood/Lymph	Murine	Non-isogenic xenograft CD7+ and CD45+ cells (human T-ALL cell)	Electron (6 MeV)	4	200	26
	Human	Spontaneous CD30+ T-cell cutaneous lymphoma	Electron (5.6 MeV)	15	1.5×10^6	35
Gut	Murine	Isogenic flank pancreatic tumor MH641905	Proton (230 MeV)	12, 15, 18	78 ± 9	24
	Murine	Isogenic flank pancreatic tumor MH641905	Proton (230 MeV)	18	112.25	43
Ovary	Murine	Orthotopic and isogenic ID8 ovarian cancer	Electron (16 MeV)	14	216	40
	Murine	Orthotopic and isogenic ID8 or UPK10	Electron (16 MeV)	14	210	42
Brain	Murine	Orthotopic and isogenic H454 glioblastoma	Electron (6 MeV)	10, 14, 25, 30	$5.6x10^6$, 1.9, 3.9, $7.8x10^6$, $2.5x10^3$, 5.6x10^6	63

Table 8. Compilation of FLASH RT tumor studies. FLASH RT achieves tumor growth control comparable to CONV RT at the same dose administered

Head & Neck	Murine	Non-isogenic xenograft Hep-2 (Human head and neck carcinoma)	Electron (4.5 MeV)	15, 20, 25	≥40	10
	Murine	Non-isogenic xenograft FaDu cells (human hypopharyngeal carcinoma)	Proton (23 MeV)	10, 15, 20, 30, 40	2×10^{10}	17
Breast	Murine	Non-isogenic xenograft HBCx-12A (human breast cancer)	Electron (4.5 MeV)	17	≥40	10
	Murine	Isogenic xenograft EMT6 mouse breast cancer	High energy X-rays	18	1000	21
	Murine	Isogenic flank C3H mouse mammary carcinoma	Proton (250 MeV)	40 - 60	83	31
	Murine	Non-isogenic, flank xenograft MDA-MB 231 (human breast cancer)	Electron (10 MeV)	10, 20, 19, 30	90, 180, 270	64

Table 8 Continued. Compilation of FLASH RT tumor studies. FLASH RT achieves tumor growth control comparable to CONV RT at the same dose administered

CHAPTER 3.

Exploring Mitochondrial Activities as a Mechanistic Explanation for the FLASH Effect

The difference between conventional and FLASH radiotherapies lies in the exposure time, where the apparent benefit of FLASH RT is in evading intrafraction organ movement during treatment (9, 11, 34, 65). However, the unexpected differential outcomes between normal and cancer cells have led the field to quest for explanations as this single difference in a physical parameter renders the four Rs of radiobiology inapplicable to explain the FLASH effect. As seen in Chapter 2 of this thesis, stem cell preservation by FLASH RT was one of the common beneficial outcomes observed across the lung, skin, blood, gut, and brain (7, 11, 26, 29, 53, 54). Several other hypotheses have been proposed, but it is outside the scope of this thesis to discuss them all (figure 2). Instead, I have focused on the oxygen depletion theory, which has been most heavily investigated and now phasing out as an improbable explanation. Then, I detail our preliminary studies on murine brain mitochondrial activities after FLASH and CONV RT to explore evidence for differential mechanisms.

Oxygen Depletion Hypothesis

Ionizing radiation results in radiochemical events that breach biological molecules such as DNA. 33% of these interactions occur via direct radiolysis that turns macromolecules into reactive radicals, which then can result in chain reactions of damaging events (8). Reasonably, the remaining 67% occurs indirectly by radiolysis of water, as water makes up more than 70% of a cell (66, 67). The resulting reactive oxygen species (ROS), such as superoxide anion radical (O2-), hydrogen peroxide (H2O2), and hydroxyl radicals

(OH·), go on to break chemical bonds of biological molecules all within an extremely short time – 10^{-15} and 10^{-12} seconds (8, 65, 68).

Radiolysis via ROS generation is the major mechanism of action, of which oxygen (O_2) acts as a potent radiosensitizer that enhances ROS production as it is consumed (8, 65, 69, 70). It has been speculated that the FLASH RT may alter this well-documented pathway via rapid depletion of oxygen, which induces transient hypoxia and, in turn, results in normal tissue protection. This hypothesis has been proposed by the earlier UHDR studies and strengthened by the carbogen breathing experiment in 2019, where increased oxygen concentration abolished the FLASH effect in the murine brain (56). The oxygen depletion hypothesis seemed plausible considering that: a) oxygen concentration is different in normal and tumor cells, which may appropriately explain the differential outcomes after FLASH RT; b) although the latter is more hypoxic, it also has 2 to 4 times the amount of labile iron that could induce damaging Fenton reactions; and c) the theoretical calculations of ROS production led to four orders of magnitude more ROS production by FLASH RT, which meant more oxygen depletion and less radiolytic damages compared to CONV RT (8). Furthermore, earlier studies from the twentieth century had experimentally shown that bacterial cell surviving fractions were highly dependent on oxygen concentration (71).

Nevertheless, in the same study, 100 Gy was required to drop oxygen concentration by a mere 3% (71). Because normal tissue protection is observed at much lower doses than 100 Gy, it is unlikely that oxygen depletion is the driving force of the FLASH effect. Moreover, the first *in vivo* experiment showed that oxygen depletion depends on the total dose rather than the dose rate, a phenomenon also reported by Weiss, 1974 (64,

71). This experimental result alone challenges the oxygen depletion hypothesis because CONV and FLASH RT should deplete oxygen at similar levels as the total dose administered is equal.

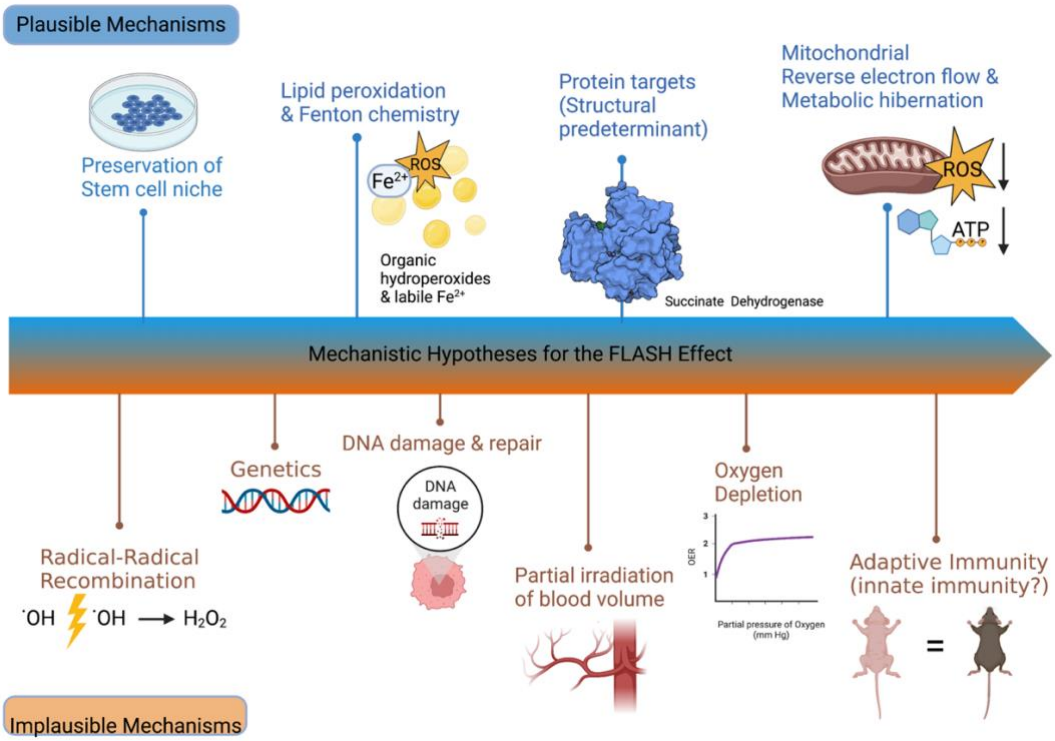

Figure 2. Overview of proposed hypotheses for the FLASH effect. (Created with BioRender.com)

Because oxygen is a potent radiosensitizer, it is reasonable that doubling the oxygen concentration by carbogen breathing eradicated the protective effects secured via FLASH RT (56). Since the generation of ROS is the main radiobiological pathway, oxygen, or the lack of it, may have some role in the FLASH effect. However, various experiments thus far have not succeeded in finding favorable evidence for this hypothesis, and the field is now looking for answers elsewhere. Our group has investigated mitochondrial activities as our mechanistic hypothesis of the FLASH effect.

Exploring Metabolic Activities post-FLASH Whole-Brain Irradiation

Background

The mitochondria are commonly deemed as the powerhouse of a cell (72, 73). Their abundance, size, shape, and activity levels vary depending on the organ systems in which they reside (74, 75). Apart from fueling life, this dynamic organelle participates in diverse cellular processes such as gene expression, steroid synthesis, apoptosis, and calcium sequestration (76, 77). Like the nucleus, the mitochondria are encapsulated by double membranes and possess their own mitochondrial DNA (mtDNA), separate from the nuclear DNA (75). Unlike nuclear DNA, mtDNA is not shielded by protective proteins, suggesting that it may be prone to radiolytic damage to a greater degree (78). Mitochondria are also the site of the most ROS production and contribute to cellular ROS homeostasis. While ROS are essential for certain signaling pathways, their imbalance due to mitochondrial dysfunction can lead to disease pathology (74, 75, 79, 80).

Mitochondria are among the common targets present across all organ types that have been summarized in Part 1 of this thesis. Tumor cells are known to have abnormal mitochondrial activities, which might contribute to the differential outcomes between normal and cancer cells by FLASH RT (81). These characteristics along with their involvement in critical cellular processes make mitochondria a reasonable target for investigation. We specifically examined murine brain metabolic activities because mitochondria are abundant and long living in this heavily energy-dependent organ (77, 82).

In the brain, ATP production is critical for maintaining concentration gradients and neurotransmitter recycling (77). Apart from the energetics, mitochondria also produce important molecular precursors for myelin synthesis and regulate calcium levels, which is particularly important at the synapse (83). Unintended calcium accumulation causes mitochondrial permeability transition, resulting in decreased ATP production and mitochondrial membrane potential, ultimately rupturing the outer mitochondrial membrane and leading to necrosis (84). Furthermore, research has shown that mitochondria are involved in autophagy and apoptotic pathways in the rat hippocampus (85). Thus, proper mitochondrial activity is critical to maintaining brain functions, as mitochondrial dysregulation has been closely associated with many neurological disease pathologies, such as Alzheimer's and Parkinson's disease (80, 82).

Given that the brain is late responding to radiation-induced injuries, neuronal mitochondria are long living and are prone to oxidative stress, and mitochondrial repair mechanisms are generally inefficient, we hypothesized that mitochondrial functions might be dysregulated at a delayed time point after CONV RT, while FLASH RT will yield results comparable to the control group (82, 87). To test our hypothesis, we measured the gross hippocampal and cortical ATP concentrations and mitochondrial fusion activities as the metabolic endpoints to discern the differences between the treatment groups at four months post-IR. This project included taking repeated measurements from two cohorts that were irradiated with a single dose of 10 Gy at different facilities. I also briefly describe the results of the XTT assay that measures mitochondrial NADH production, but was abandoned as inadequate for our investigation's purposes.

Methodology

XTT Assay

XTT assay is an *in vitro* assay traditionally used to detect cell proliferation of tumor cells to test drug efficacy where Tetrazolium dye (XTT in short) reacts with electrons from a high energy electron carrier NADH produced by mitochondria and yields formazan, an orange-colored product (figure 3). We explored possibilities of exploiting this simple yet informative assay to compare the metabolic activities between CONV and FLASH-irradiated brain tissue samples (Abcam XTT Assay Kit, ab232856). We hypothesized that CTL and FLASH groups would be comparable, while CONV RT would significantly reduce colorimetric changes. We ran two test rounds to verify whether whole or minced tissues worked better for this test and identified an inert buffer that best preserved mitochondrial activities.

ATP Assay

ATP determination is a simple assay that informs metabolic activities and general mitochondrial health (74, 80). Differences in the ATP output compared to the control group would indicate physiological changes and incentivize deeper investigation. Decreased ATP output can be expected if the electron transport chain (ETC) mitochondrial proteins are damaged (88). We hypothesized that the ATP levels of CTL and FLASH RT would be comparable, while significantly different following CONV RT compared to CTL and FLASH irradiated groups.

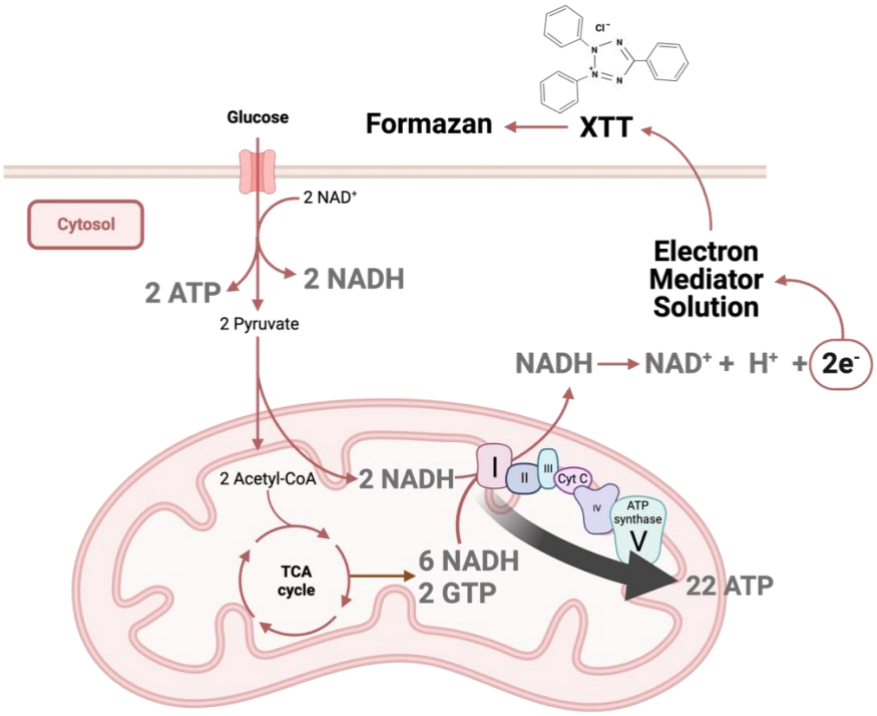

Figure 3. Schematic of mitochondrial energetics. The XTT colorimetric change reflects mitochondrial NADH production, whereas the ATP assay measures the overall energy output by the mitochondria (Created with BioRender.com)

Assessing Mitochondrial Dynamics via OPA-1

Mitochondria are not only functionally dynamic but structurally interesting as they constantly undergo fission and fusion in response to the changes of the cellular environment – a phenomenon referred to as mitochondrial dynamics (figure 4) (76, 80). Although excessive mitochondrial fission (or fragmentation) is commonly associated with many neurodegenerative diseases such as Alzheimer's, Parkinson's, Huntington's, proper balance between fission and fusion is necessary for the survival of nonproliferating neurons (80, 89).

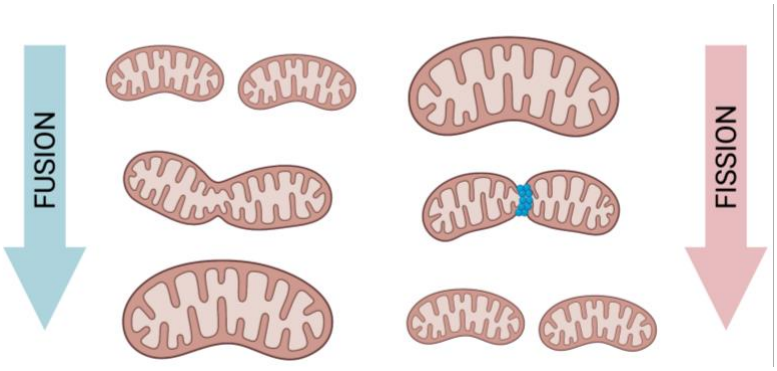

Figure 4. Mitochondrial dynamics depicting fusion and fission activities (Created with BioRender.com)

Mitochondrial fusion is a built-in stress response against factors such as radiation or increased energy demand of the cell. During this process, damaged mitochondria combine with the undamaged to mix up metabolites and increase mtDNA copy number, thereby adequately enhancing the capacity for stress modulation (80, 89). Fusion activity results in larger mitochondrial size, which is associated with ATP outputs (90). Optic atrophy-1 (OPA-1) is an inner mitochondrial membrane fusion protein that can inform about mitochondrial energy outputs, stress levels, and overall health (80). OPA-1 exists in several variants, of which the two main isoforms are long and short-OPA1. Long-OPA1 (L-OPA1, ~100 kDa) is associated with mitochondrial fusion. L-OPA1 processing via cleavage at S1 site results in short-OPA1 (S-OPA1, ~75 kDa), which is associated with fission (90, 91, 92). Under normal conditions, these isoforms exist at a roughly equal concentration (91). L-OPA1 is depressed (by cleavage resulting in S-OPA1) when ATP concentration is low and oxidative stress is increased. S-OPA1 is increased as a cellular survival mechanism (90). Therefore, concentrations of L-OPA1 and S-OPA1 and the ratio of the two can all provide useful insight into mitochondrial functions.

Considering cognitive decline post-CONV RT is progressive and causes more oxidative stress and radiolytic damage than FLASH RT, we hypothesized that mitochondrial ATP production would be altered, S-OPA1 would be elevated, and/or L-OPA1 would be depressed if there is progressive and lasting mitochondrial dysregulation at four months after CONV irradiation. We also expected to see that our L-OPA1 data would have a positive association with the ATP output and S-OPA1. Finally, any departure from the normal 1:1 L-OPA1:S-OPA1 ratio at four months would inform that WBI induces lasting changes in mitochondrial dynamics.

Materials and Methods

Animals and Irradiation

All animal experiments were approved by the Swiss ethics committee (VD3603) and the Institutional Animal Care and Use Committee at the University of California, Irvine (IACUC, AUP- 21-025) and Stanford University, CA (APLAC-27939). At Stanford, 11 to 12 weeks old C57B1/6J female mice were purchased from the Jackson Laboratories (n=18). The animals were allowed to acclimate before receiving 10 Gy whole-brain irradiation (WBI) under isoflurane anesthesia (3% for induction, 2% for maintenance, in room air) to ensure accurate delivery of radiation to the brain. At Stanford, conventional dose was delivered at 0.1 Gy/s. The FLASH irradiation was given in five pulses (≤0.05 seconds). The dose rate per pulse was 5.3×10^5 Gy/s, and the mean dose rate was 225 Gy/s. At Lausanne University Hospital (CHUV), 11 weeks old C57B1/6J female mice received 10 Gy WBI at a conventional dose rate of 0.1 Gy/s. The FLASH irradiation was given in a single pulse in 1.8 microseconds. The instantaneous dose rate

was 5.6 $\times$ 10^6 Gy/s. The irradiation modalities at Stanford and CHUV were performed as previously published (57, 58).

The animals were monitored daily for body weight, appearance, and respiratory rate during the first week, and every other day afterwards until transported to the University of California, Irvine at three weeks post-irradiation. The animals were housed under standard conditions (20°C ± 1°C; 70% ± 10% humidity; 12:12 h light-dark schedule) with access to standard rodent chow and water *ad libitum* until metabolic investigations were performed at four-months after treatment.

Perfusions and Tissue Collection

Mice were treated with isoflurane anesthesia prior to brain perfusion and surgery. 25 mL of heparinized saline-on-ice was injected into the left ventricle of the heart for intracardial brain perfusion via a Peri-Stare™ Pro peristaltic pump (World Precision Instruments, Sarasota, FL). Fixation agents (i.e., 4% paraformaldehyde (PFA) were not used to maintain mitochondrial activities as closely as possible to the biological state. Two hippocampi and two frontal cortical tissues were harvested on ice. The tissues were each placed in cold 150 ul of 1x RIPA lysis buffer (sc-24948, Santa Cruz Biotech), homogenized using a motorized tissue homogenizer, and put on ice for 20 minutes before spun at 13,000 rpm at 4°C for 30 minutes. Supernatants were transferred to 1.5 ml Eppendorf tubes on ice and processed for Bradford and ATP assays right away. Remaining lysates were stored at -80°C for Western blot analysis of OPA-1.

Bradford Assay

Standard Bradford assay protocol was followed to measure sample protein concentrations (Bio-Rad Protein Assay Kit I #5000001). In brief, 20 mg/ml bovine serum

albumin (BSA) stock solution was used to make a protein concentration standard curve (0, 1.25, 2.5, 5, 10 ug/ul). All standard solutions and samples were added to each well of a 96-well plate with 25 ul of Bio Rad reagent A (Cat#: 500-0113) and 5 ul of reagent S (Cat#: 500-0115). 200 ul of Bio Rad reagent B was added the last. The plate was read with BioTek, SynergyMx plate reader (Gen5.v1.11), at 595 nm to determine the sample protein concentrations.

XTT Assay

Whole hippocampus, minced hippocampus, remaining minced brain tissue were placed in 100 ul PBS buffer. PBS buffer served as a negative control (figure 5). Each sample was treated with 10 ul of XTT reagent prepared by combining equal volumes of XTT Developer Reagent and Electron Mediator solutions. Initial absorbance at 450 nm optical density was measured using BioTek, SynergyMx plate reader (Gen5.v1.11). The samples were incubated at 37°C in a 5% CO_2 incubator until further readings were taken at 30-, 60-, 90-, and 120-minute time points. Next, we identified the buffer type most appropriate for our *in vivo* assay by testing reaction potentials in commercial PBS, HEPES, IMDM, and respiration buffer made in-house (Thermo Fisher Scientific). All the buffers were transparent without the phenol red content. Respiration buffer was prepared by combining the following: 8.4 ml MilliQ water, 0.684 g sucrose, 1 ml Tris HCl (0.1M), 0.5 ml PBS (0.1M), 4 ul EDTA (0.5 M), and 50 ul KCl (4 M). One control mouse was sacrificed, and half of left and right hippocampus and cortex samples were used. Measurements were taken in 20-minute increments for two hours. Tissue weight was measured as a mean to standardize data but was found inadequate, as extra water weight from condensation made the weight measurements unreliable. 300 μm tissue

biopsy punch and brain sectioning tools were used to standardize our final round of XTT assay with CONV and FLASH-irradiated animals (Zivic Instrument, PUN0300). 1x PBS buffer was used in the reaction.

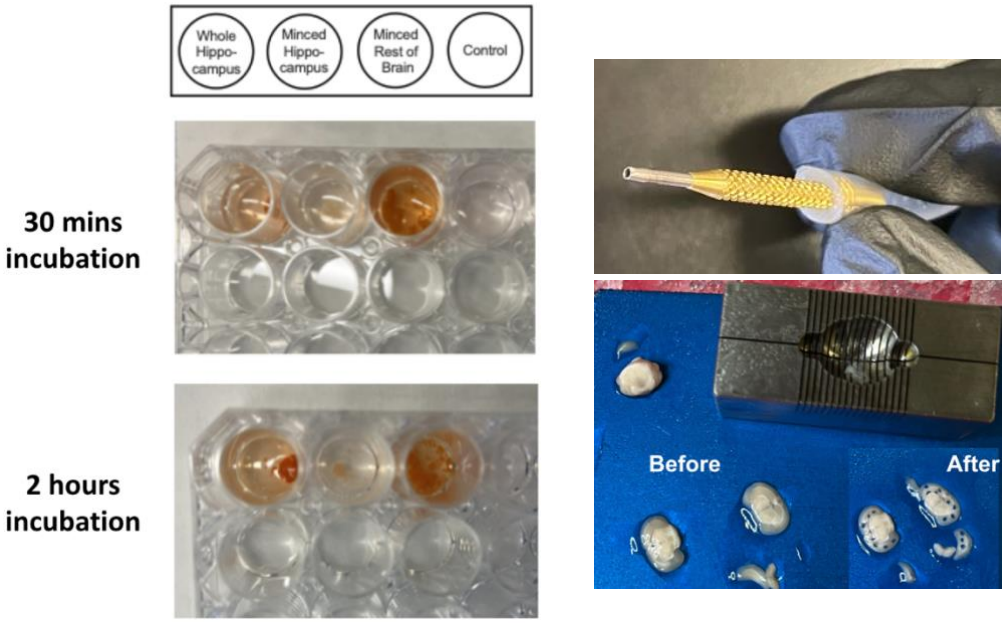

Figure 5. Preliminary in vivo XTT study setup. Left: determining reaction capacity based on different tissue types; right: tissue collection is performed via biopsy punch

ATP assay

ATP levels of fresh murine hippocampal and cortical lysates were determined via an ATP determination kit (Invitrogen A22066). Each tissue slice was considered as a sample, resulting in n=12 with 6 animals per treatment group. ATP reaction solution was prepared following the kit instruction and kept on ice and away from light until and during use. 450 ul ATP reaction solution and 50 ul ATP standard or samples were seeded per well. Each plate consisted of one set of ATP standard solutions (ranging from 0, 10, 50, 100, 200, and 500 nM), and luminescence was taken via BioTek, SynergyMx plate reader (Gen5.v1.11). Finished reaction solutions were removed prior

to running the next set of readings. One sample (hippocampus or cortex) from each of the three treatment group animals (CTL, CONV, and FLASH RT) was read concurrently (figure 6). All standard curves had high R^2 values above 0.9. The data were normalized to control prior to statistical analyses.

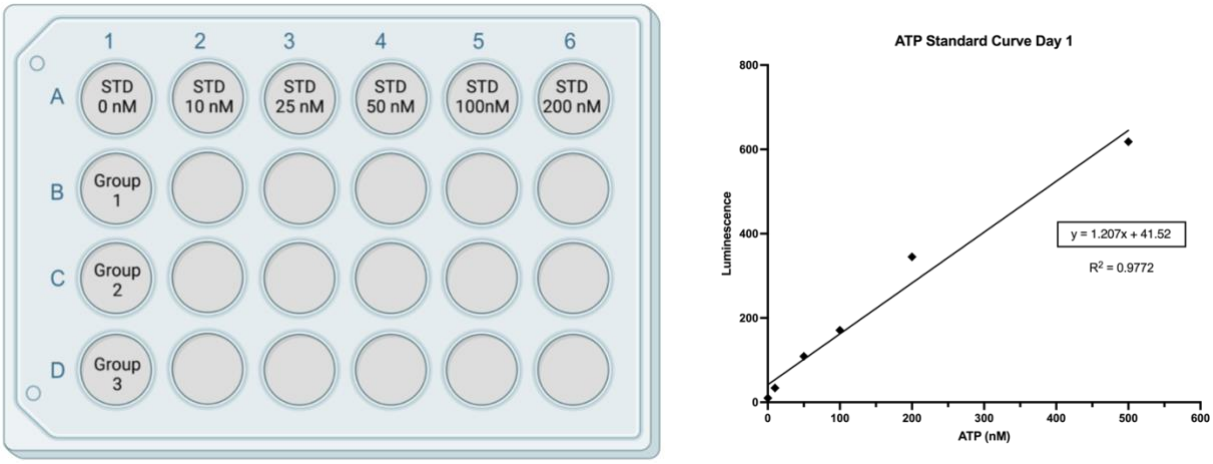

Figure 6. Set up for an ATP assay. Left: a representative loading of ATP samples in a 24-well plate; right: a representative ATP standard curve (Created with BioRender.com)

Western Blot

Western blot of OPA-1 mitochondrial fusion marker was performed following standard protocol (Invitrogen, AB_11153569). Only the left hippocampus and cortex samples were analyzed (n=6 per tissue type). Samples were thawed on ice and prepared by combining 6 ul loading dye, 50 ug of proteins calculated from Bradford assay, and variable volume of lysis buffer to result in 35 ul total volume. Samples were mixed well, spun, and boiled at 100°C for 5 minutes using a PCR cycler (BioRad), then kept at -20°C and spun before use.

1.5 mm-thick 10% separating gel was prepared by combining 2.4 ml dH_2O, 5 ml 2x separating buffer (45.5 g 375 mM Tris base and 1 g 0.1% SDS), 2.5 ml 40%

acrylamide/bis (29:1), and 66 ul 12.5% APS on ice, and vortexed to mix. 34 ul 100% TEMED was added and vortexed well to mix. The gel solution was poured into the Western blot glass assembly and 1 ml of dH_2O was added to remove bubbles and form a straight line at the top. Once the gel solidified, water was removed.

1.5 mm-thick 4% stacking gel was prepared by combining 1.35 ml dH_2O, 1.88 ml 2x stacking buffer (2x stock, 100 ml, 3.03 g 125 mM Tris base and 0.2 g 0.1% SDS), 0.51 ml 40% acrylamide/bis (29:1), and 15 ul 12.5% APS on ice and vortexed well. 12 ul 100% TEMED was added and vortexed well to mix and poured into the glass assembly. 50 ul comb was placed. The gel assembly was placed in the Western blot chamber filled with running buffer (990 ml 1x TG and 10ml 10% SDS) and ran for 1.5 hours at 100 V. Gel transfer apparatus was set up in the order following: anode, sponge, 3 Whatman paper, membrane, gel, 3 Whatman paper, sponge, and cathode. Transfer buffer (100 ml 10x TG, 200 ml methanol, and 700 ml dH_2O) was poured and run at 220 mA for 1.5 hours.The samples were washed with washing buffer (100 ml 10x ST, 1 ml TWEEN, 899 ml dH_2O) and blocked on a shaker for 1 hour in a blocking solution (5g dry milk in 100 ml washing buffer). Samples were washed with washing buffer and 1:1000 OPA-1 and 1:5000 beta-actin in 1.5% BSA/washing buffer were added. Samples were left overnight on a shaker at 4°C. The following day, the membranes were washed three times for 5 minutes each. 1:5000 goat a-rabbit and 1:5000 goat a-mouse secondary antibodies were added in 1.5% BSA/washing buffer and left on shaker away from light for one hour until samples were retrieved for imaging via Li-Cor Image system (Li-Cor, 926-68071).

Statistical analysis and study limitation

ATP data were standardized to protein concentration, and OPA-1 readings were standardized to actin concentration before normalizing the data to the control group for statistical tests. The R program (version 4.3.0) was used to assess the assumptions for one-way ANOVA and Pearson's correlation. Shapiro-Wilk normality test was employed for our small sample size ($n \leq 50$) and Bartlett's test was used to evaluate the equal variance of residuals. Data violating the normality assumption were log-transformed prior to conducting one-way ANOVA test with Bonferroni correction. Pearson's correlation analysis was performed to assess the relationships between the L-OPA1 and S-OPA1 isoforms in each treatment group. The differences in R-values across the treatment groups were assessed by performing Fisher Z-transformation, and the statistical significance was determined using a two-tailed T-test criteria, where the resulting values less than -1.96 or greater than +1.96 were considered significantly different. Graphs were generated using the R program and the GraphPad Prism software (Graphpad Software Inc, San Diego California, USA, version 9.4.1). Lastly, post hoc power analyses were performed using the G*Power program to evaluate our study's statistical power (version 3.1). A priori power analysis via Exact Correlation Bivariate Normal Model Test was performed using the R^2 values from our results as the effect size.

Results

XTT Assay

One of the questions we aimed to address was whether the *in vitro* XTT assay could yield colorimetric changes in brain tissue samples. Our results confirmed that brain tissue samples could be used with this assay, and whole brain sections allowed for

more pronounced reactions than the minced tissues. The samples in PBS and respiration buffers yielded the most stable reactions that plateaued over the two hours of the incubation period, while IMDM cell culture media with high glucose content showed a constant increase and an abrupt spike at the end of data collection (figure 7). Hence, we chose the commercial PBS buffer for our experiment. As expected, the reaction level in negative control brain tissue was significantly lower compared to freshly harvested control, CONV, and FLASH-irradiated brain sections ($p<0.0001$) (figure 7).

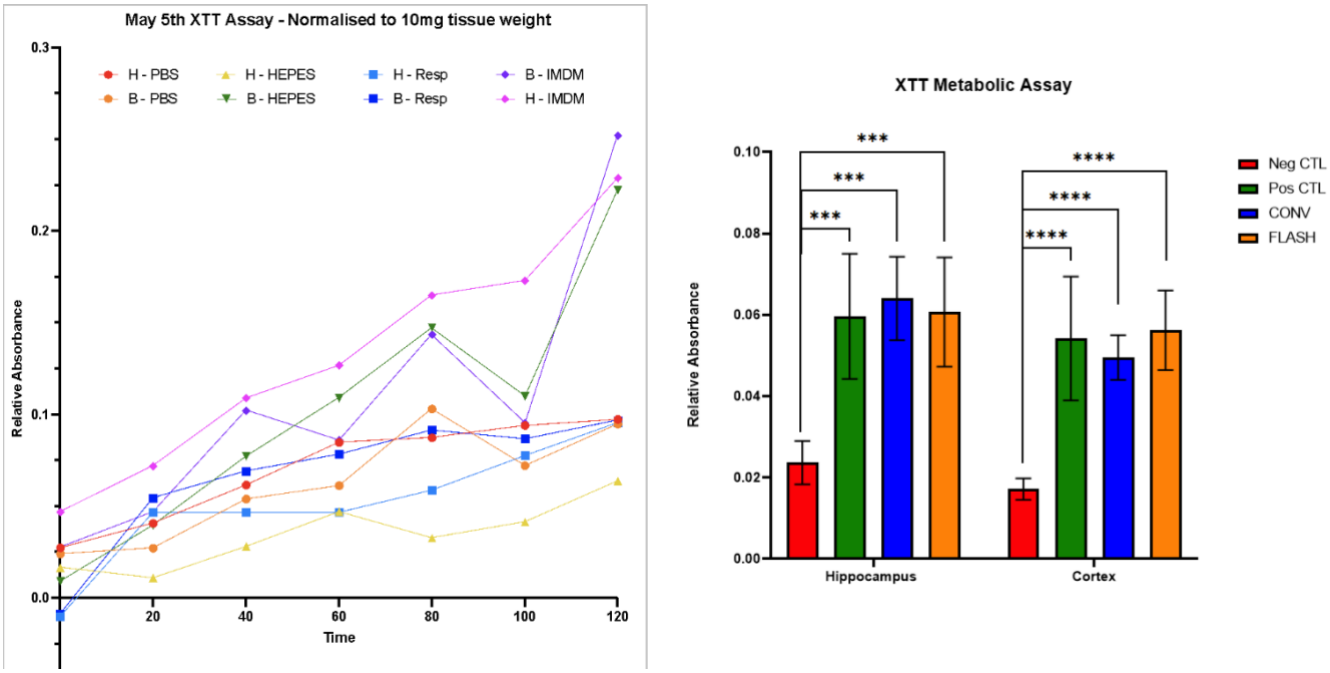

Figure 7. Preliminary results of in vivo XTT assay. Left: colorimetric changes of half hippocampus (H) and cortex (B) samples of a control mouse in four buffer types. The measurements were taken over a two-hour CO2 incubation period, with commercial PBS buffer ultimately selected for use; right: preliminary experimental results depicting the colorimetric changes observed in negative control, CTL, CONV, and FLASH irradiated groups (n=3)

Given the small sample size, no significant differences were observed across the treatment groups (n=3; $p>0.9$). The difficulty in standardizing the results led us to

abandon the use of this assay for our project's purposes. Future studies may find Bradford assay useful for standardizing after the assay has taken place.

ATP Assay

We measured the overall ATP output from the hippocampus and frontal cortex tissues to assess the general state of mitochondrial functions. Each side of the tissue sections was considered as a sample (hence, n=12 from 6 mice per group). There was no significant difference in ATP concentration among the treatment groups, although the CHUV cohort exhibited a stronger trend toward statistical significance compared to the Stanford cohort (figure 8, table 9).

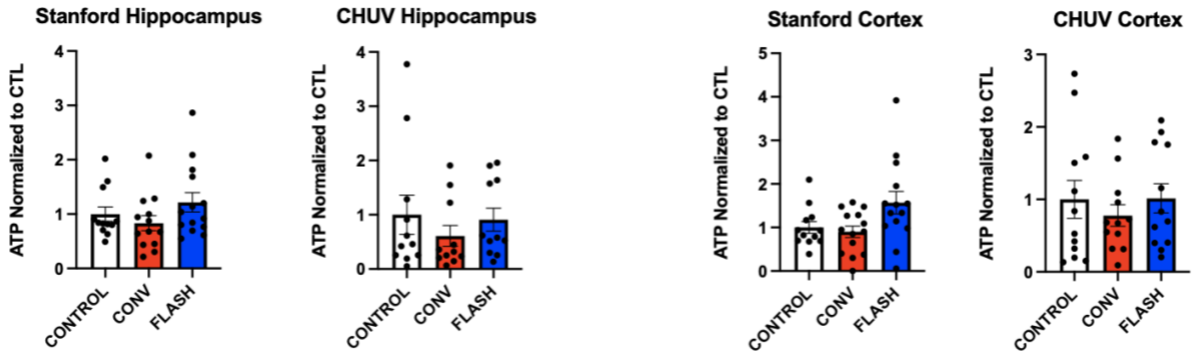

	Stanford Hippocampus	CHUV Hippocampus	Stanford Cortex	CHUV Cortex
CTL-CONV	p=0.60	p=1.0	p=1.0	p=1.0
CTL-FLASH	p=1.00	p=1.0	p=0.126	p=1.0
CONV-FLASH	p=0.12	p=0.68	p=0.067	p=1.0

Figure 8. ATP output normalized to the CTL after a single 10 Gy sham, conventional, and FLASH irradiation (n=14 for CONV and FLASH RT, n=12 for CTL due to missing data)

Cohort	Treatment group	Hippocampus vs. Cortex (p-value)
Stanford	**CTL**	0.27
	CONV	0.924
	FLASH	0.967
CHUV	**CTL**	0.162
	CONV	0.0865
	FLASH	0.0712

Table 9. The statistical differences in ATP output between the brain regions within each treatment group. The Stanford cohort exhibited a stronger lack of difference than the CHUV cohort

Western blot of OPA-1

Mitochondrial fusion marker OPA-1 expression was measured to assess mitochondrial dynamics, stress response, and its relationship with ATP production. First, we compared the OPA-1 protein expressions by tissue types and cohorts among the treatment groups. The individual levels of L-OPA-1, S-OPA1, and isoform ratio did not exhibit statistical differences across the treatment groups, as depicted in Figure 9. These measures were further compared with the previously collected ATP data via Pearson's correlation analysis.

ATP output is associated with mitochondrial dynamics. To assess this relationship, correlation strengths between [ATP] and L-OPA1 were compared across the treatment groups (figure 10). Since both ATP and L-OPA1 levels did not statistically differ between the hippocampus and cortex, combined data were used (n=12). Stanford and CHUV cohorts resulted in opposing direction of associations between ATP and L-OPA1 expressions, but these relationships (denoted by the R-values) were not statistically significant ($p>0.05$). The R-values did not significantly differ between control and test groups across the cohorts (table 10).

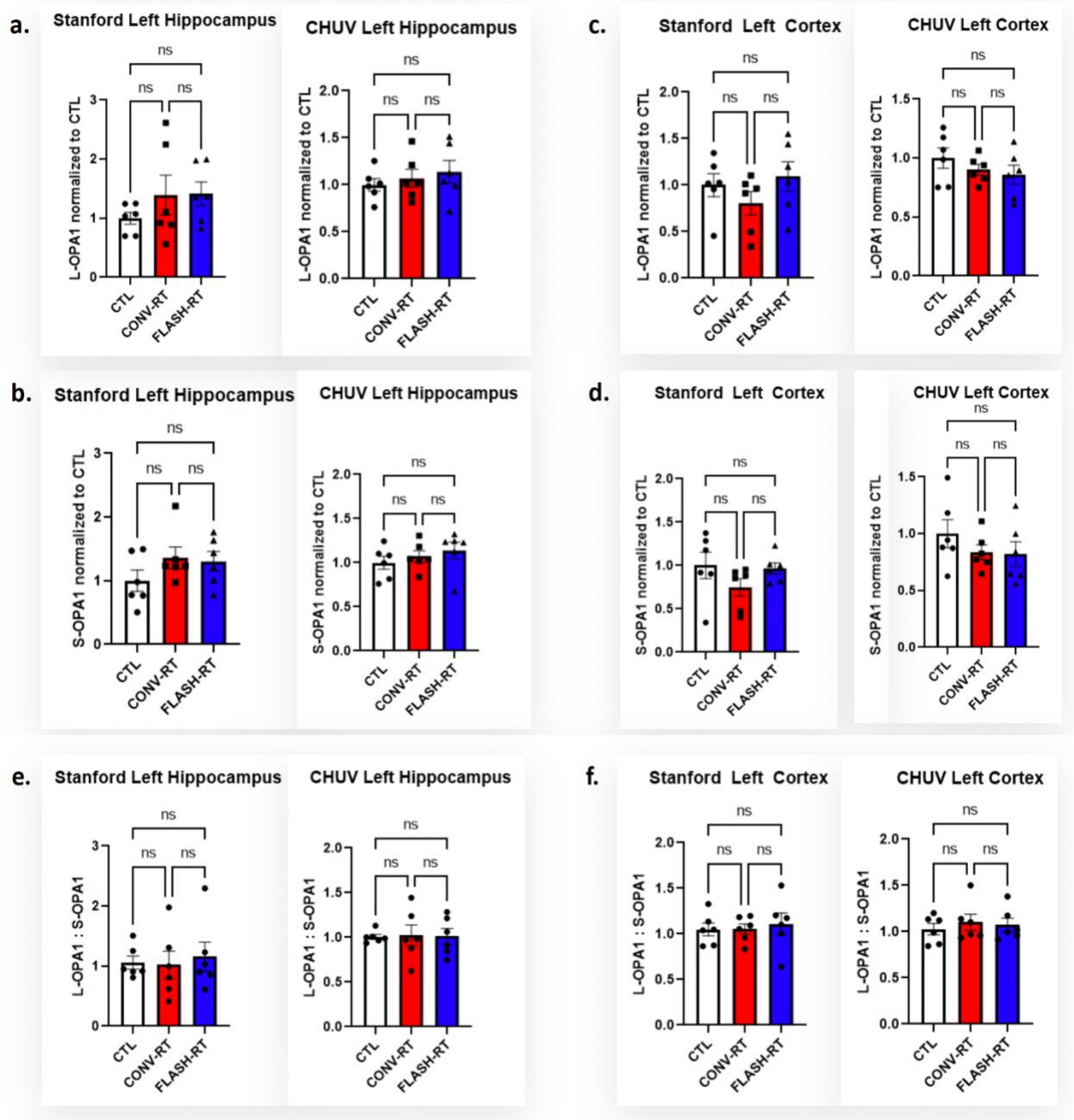

Figure 9. L-OPA1 and S-OPA1 expressions of a-b) the left hippocampi from both cohorts; c-d) the left cortex from both cohorts; e-f. L-OPA1 to S-OPA1 ratios for hippocampus and cortex samples from both cohorts, not normalized to control

Next, the association between [ATP] and S-OPA1 expressions were analyzed.

Interestingly, Stanford CONV and FLASH groups expressed significantly different S-OPA1 levels between the tissue types (p=0.00595 and 0.015, respectively). The CONV

and FLASH CHUV animals likewise exhibited differences (p=0.0295 and 0.0516, respectively). Thus, the S-OPA1 data of these groups were separated by tissue types to run the analyses (n=6). CTL groups from both cohorts did not exhibit such differences in S-OPA1 expressions; hence, CTL data were combined for comparisons via Fisher z-transformation (n=12).

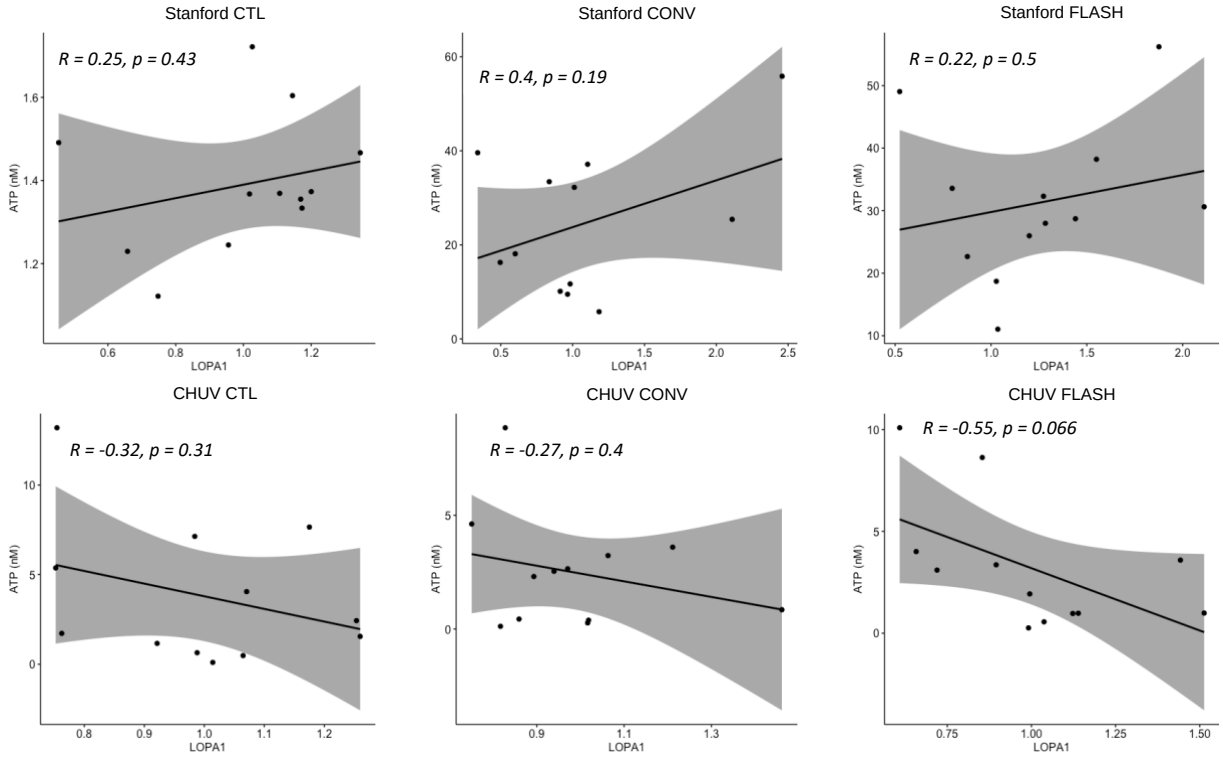

Figure 10. Correlation analysis between ATP output and L-OPA1 expression in each treatment group at 4 months after a single 10 Gy irradiation. Data points from the hippocampus and cortex were combined (n=12)

Similar to the [ATP] and L-OPA1 results, the [ATP] and S-OPA1 relationship did not vary across the cohort and treatment groups. The data did not present sufficient evidence to conclude that ATP is associated with individual L-OPA1 or S-OPA1 expressions.

	p-value
Stanford CTL-CONV	0.722
Stanford CTL-FLASH	0.946
Stanford CONV-FLASH	0.671
CHUV CTL-CONV	0.908
CHUV CTL-FLASH	0.543
CHUV CONV-FLASH	0.469
Stanford CTL-CHUV CTL	0.213
Stanford CONV-CHUV CONV	0.137
Stanford FLASH-CHUV FLASH	0.074

Table 10. Statistical comparisons for ATP concentration and L-OPA1 expression correlation analyses between the treatment groups within and across two cohorts

The relationship between L-OPA1 and S-OPA1 was then analyzed. Under normal conditions, L-OPA1 and S-OPA1 ratio is balanced at roughly 1:1, where S-OPA1 is derived from L-OPA1 cleavage. Both CTL groups from Stanford and CHUV cohorts had an equally strong positive correlation between the isoforms ($r(10)=0.9$, $p=6.6 \times 10^{-5}$) (figure 10). All but one cortex tissue samples exhibited similarly strong positive relationships that were also statistically significant ($p<0.05$). Conventionally irradiated CHUV cortex samples displayed a weaker and nonsignificant association but maintained a positive relationship ($r(4) = 0.48$, $p = 0.34$). The L-OPA1:S-OPA1 relationships of all cortex tissues did not differ significantly from those of the CTL group. On the other hand, Stanford FLASH and CHUV CONV irradiated hippocampus samples exhibited significantly different relationships of the isoforms compared to the CTL group ($p = 0.005$ and $p = 0.012$, respectively). While the strengths of associations (R) were weaker than their cortex counterparts across the cohorts, only the Stanford CONV and FLASH irradiated groups showed significant and marginally significant differences compared to the cortex ($p = 0.0496$ and 0.057, respectively).

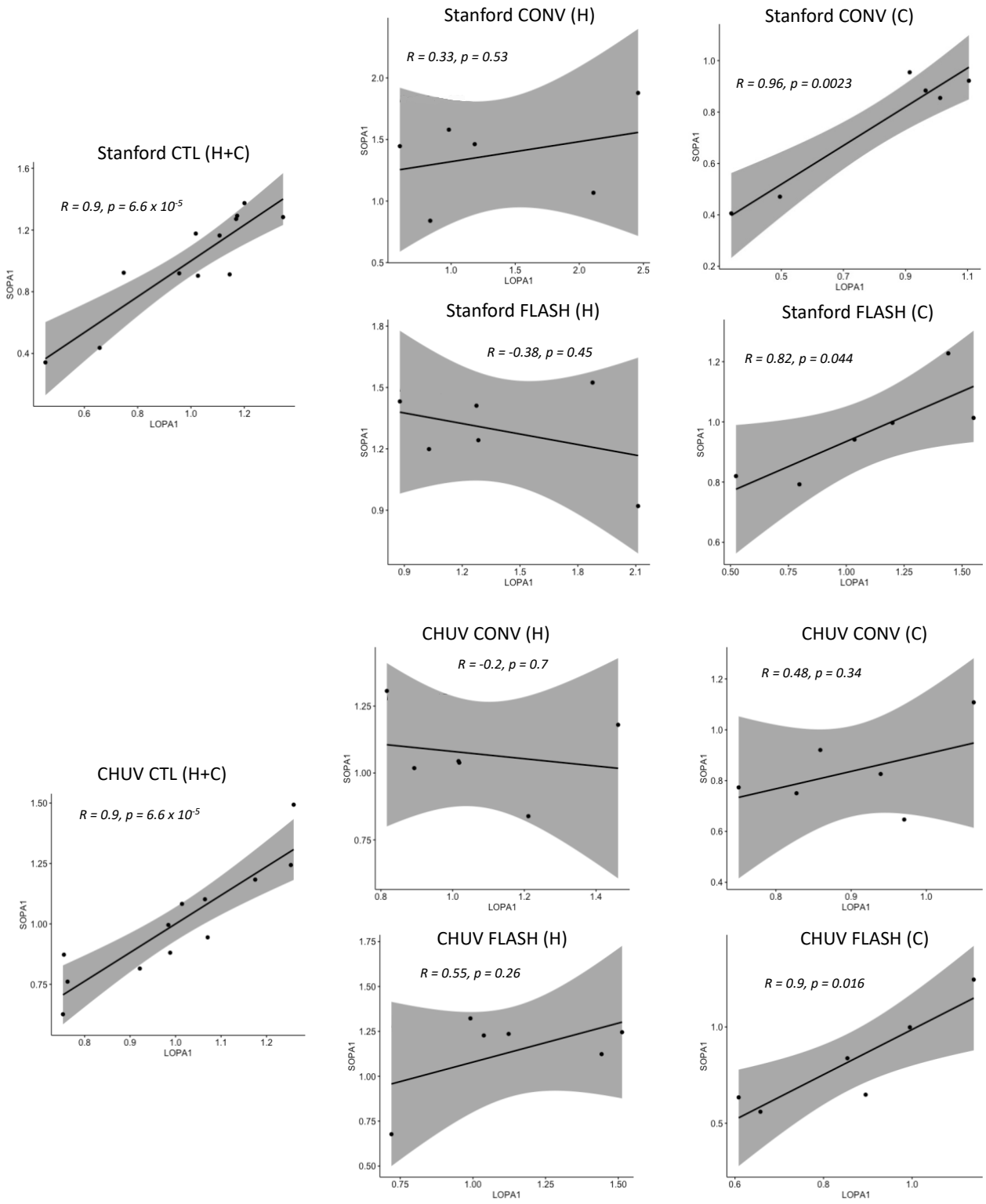

Figure 11. Correlation analyses of L-OPA1 and S-OPA1 isoforms by cohorts, treatment groups, and tissue types. (H+C): hippocampus and cortex combined (n=12), (H): hippocampus (n=6), (C): cortex (n=6).

Lastly, [ATP] was compared against the L-OPA1:S-OPA1 ratio to explore the associations between ATP and mitochondrial dynamics. No significant association was found between ATP and OPA-1 isoform ratios across the cohorts, treatment groups, and tissue types within our cohorts at four months post-IR.

Discussion

Following the first publication about FLASH radiotherapy and its extraordinary normal tissue sparing, numerous *in vivo* experiments have consistently confirmed the FLASH effect across species, organ types, and radiation modalities. These studies have demonstrated reduced inflammation, fibrosis, and stem/progenitor cell preservation as typical protective outcomes across the organ systems (7, 10, 22, 29, 32, 36, 39, 58). Ultrahigh dose rate FLASH radiotherapy inherently reduces exposure time and attenuates normal tissue toxicity, perhaps, due to minimized disruptions to cellular processes. Alongside this advantage, FLASH microbeam irradiation (FLASH MRT) reduces exposure area, which has shown potential for administering even greater doses (300 and 600 Gy) while maintaining normal lung tissue toxicity comparable to that of a 30 Gy traditional FLASH RT beam (22). While future studies need to confirm the cancer treatment efficacy of FLASH MRT, these results, along with a hypo-fractionated FLASH RT dose regimen, may be potential avenues for further widening the radiotherapeutic window considering that tumor growth control directly depends on the total dose administered (22, 63).

Before FLASH RT transitions to clinical practice, long-term toxicity must be addressed. Since most organismal FLASH RT studies have utilized mouse models, the observational periods have primarily remained under a year. The study by Rohrer Bley

et al. extended the follow-up period after a 30 Gy FLASH irradiation (1500 Gy/s) of feline skin cancer patients (33). The researchers reported severe bone necrosis at 12 and 15 months, an outcome not previously observed in murine studies, highlighting the necessity to reevaluate the effects of FLASH RT treatment on each organ type.

The ongoing question in the field has been the search for mechanistic explanations of the FLASH effect, as the most prominent oxygen depletion theory is waning due to the lack of experimental evidence (64, 71). Previous studies have reported that FLASH RT reduces DNA DSB, cytokine expression, and inflammatory pathways at the cellular level (7, 29, 30, 38, 57, 62). Yet, the impact of FLASH RT on mitochondria and bioenergetics has not been explored. To address this gap in the field, we investigated mitochondrial activities as a potential explanation for the lasting FLASH effect in the murine brain.

In the brain, mitochondrial dynamics are closely involved with neurodegenerative disease pathologies (80, 82). Considering that the mitochondria are dysregulated in cancer cells and involved in critical cellular pathways such as apoptosis, this organelle was a reasonable target of our investigation (81). We evaluated the metabolic capacities and mitochondrial dynamics in the murine hippocampus and cortex as the endpoints to verify the mitochondrial physiology 4 months after FLASH and conventional dose-rate irradiations.

L-OPA1 and S-OPA1 isoforms exist at roughly 1-to-1 ratios, where S-OPA1 results from L-OPA1 cleavage (91). To explore this relationship, we performed Pearson’s correlation analysis. Consistent with expectations, the CTL groups from both Stanford and CHUV cohorts showed robust positive relationships between the two isoforms. While the similar pattern was also reflected across the cortex tissues, the hippocampus

manifested weaker associations where Stanford FLASH and CHUV CONV irradiated groups significantly differed from their CTL group. These results may indicate that 10 Gy CONV and FLASH RT potentially dysregulate mitochondrial dynamics in the hippocampus that can still be observed four months after irradiation.

As observed from our study, some level of damage in the hippocampus by FLASH RT is not unexpected. We have seen from Section 2.7 that both radiotherapies resulted in toxicity. For example, FLASH RT significantly depressed hippocampal neurogenesis, although to a lesser degree than CONV RT (20, 54). In our case, however, we did not have sufficient statistical power to detect potential differential responses between CONV and FLASH dose rates. In future studies evaluating the mitochondrial dynamics with OPA-1 isoforms, we recommend using a sample size of at least 14 to achieve 80% power (a priori power analysis with $\alpha = 0.05$, $\beta = 0.8$, and the effect size of 0.6724 derived from Stanford FLASH cortex – the lowest R^2-value).

Contrary to our alternative hypothesis, there were no significant differences at the individual levels of ATP, L-OPA1, S-OPA1, and isoform ratios. The absence of statistical findings for ATP output can be attributed to its close association with cell survival and tight regulation as demonstrated by compensatory mechanisms, such as fumarate serving as the terminal electron acceptor under suboptimal conditions (93). Based on our preliminary results, the significant difference in L-OPA1 and S-OPA1 relationships in the hippocampus after CONV and FLASH irradiations compared to control indicate that the mitochondria may be an adequate target for further investigation.

Future studies should use more refined tests for ATP determination and mitochondrial activities (e.g., liquid chromatography mass spectrometry, RNA sequencing) to determine whether the mitochondria are involved in effecting the differential responses between FLASH and CONV radiotherapies. Other considerations might be to explore the potential connection between mitochondrial performance and the manifested behavior at the organismal level. Moreover, mitochondrial translocation is a critical factor that should be evaluated along with assessing mitochondrial functions in the murine brain. The mitochondria actively move along the axons and must be at the site of energy demand because ATP does not diffuse well (77). Compromised mitochondrial transport due to damaged cytoskeletons can result in inadequate calcium sequestration and ATP production at the site of demand, ultimately damaging the neurons. The neurofilament light chain is a blood marker of immunoassay that could help evaluate cytoskeleton damage post-irradiation (94, 95). Finally, another alternative approach could be to test for a specific marker of mitochondrial damage (e.g., NLRP10 in skin tissues) to directly evaluate the impact of conventional and FLASH radiation therapies on mitochondrial physiology (96). This assessment could more clearly elucidate the relevance (or the lack thereof) of mitochondrial activities to the mechanistic explanations for the FLASH effect.

REFERENCES

1. Ugai, T., Sasamoto, N., Lee, H. Y., Ando, M., Song, M., Tamimi, R. M., Kawachi, I., Campbell, P. T., Giovannucci, E. L., Weiderpass, E., Rebbeck, T. R., & Ogino, S. (2022). Is early-onset cancer an emerging global epidemic? Current evidence and future implications. Nature reviews. Clinical oncology, 19(10), 656–673. https://doi.org/10.1038/s41571-022-00672-8

2. Siegel, R. L., Miller, K. D., Fuchs, H. E., & Jemal, A. (2021). Cancer Statistics, 2021. CA: a cancer journal for clinicians, 71(1), 7–33. https://doi.org/10.3322/caac.21654

3. Schaue, D., & McBride, W. H. (2015). Opportunities and challenges of radiotherapy for treating cancer. Nature reviews. Clinical oncology, 12(9), 527–540. https://doi.org/10.1038/nrclinonc.2015.120

4. Baumann, M., Krause, M., Overgaard, J., Debus, J., Bentzen, S. M., Daartz, J., Richter, C., Zips, D., & Bortfeld, T. (2016). Radiation oncology in the era of precision medicine. Nature reviews. Cancer, 16(4), 234–249. https://doi.org/10.1038/nrc.2016.18

5. Vozenin, M. C., Bourhis, J., & Durante, M. (2022). Towards clinical translation of FLASH radiotherapy. Nature reviews. Clinical oncology, 19(12), 791–803. https://doi.org/10.1038/s41571-022-00697-z

6. Connell, P. P., & Hellman, S. (2009). Advances in radiotherapy and implications for the next century: a historical perspective. Cancer research, 69(2), 383–392. https://doi.org/10.1158/0008-5472.CAN-07-6871

7. Fouillade, C., Curras-Alonso, S., Giuranno, L., Quelennec, E., Heinrich, S., Bonnet-Boissinot, S., Beddok, A., Leboucher, S., Karakurt, H. U., Bohec, M., Baulande, S., Vooijs, M., Verrelle, P., Dutreix, M., Londoño-Vallejo, A., & Favaudon, V. (2020). FLASH Irradiation Spares Lung Progenitor Cells and Limits the Incidence of Radio-induced Senescence. Clinical cancer research : an official journal of the American Association for Cancer Research, 26(6), 1497–1506. https://doi.org/10.1158/1078-0432.CCR-19-1440

8. Spitz, D. R., Buettner, G. R., Petronek, M. S., St-Aubin, J. J., Flynn, R. T., Waldron, T. J., & Limoli, C. L. (2019). An integrated physico-chemical approach for explaining the differential impact of FLASH versus conventional dose rate irradiation on cancer and normal tissue responses. Radiotherapy and oncology : journal of the European Society for Therapeutic Radiology and Oncology, 139, 23–27. https://doi.org/10.1016/j.radonc.2019.03.028

9. Vozenin, M. C., Hendry, J. H., & Limoli, C. L. (2019). Biological Benefits of Ultra-high Dose Rate FLASH Radiotherapy: Sleeping Beauty Awoken. Clinical oncology (Royal College of Radiologists (Great Britain)), 31(7), 407–415. https://doi.org/10.1016/j.clon.2019.04.001

10. Favaudon, V., Caplier, L., Monceau, V., Pouzoulet, F., Sayarath, M., Fouillade, C., Poupon, M. F., Brito, I., Hupé, P., Bourhis, J., Hall, J., Fontaine, J. J., & Vozenin, M. C. (2014). Ultrahigh dose-rate FLASH irradiation increases the differential response between normal and tumor tissue in mice. Science translational medicine, 6(245), 245ra93. https://doi.org/10.1126/scitranslmed.3008973

11. Vozenin, M. C., De Fornel, P., Petersson, K., Favaudon, V., Jaccard, M., Germond, J. F., Petit, B., Burki, M., Ferrand, G., Patin, D., Bouchaab, H., Ozsahin, M., Bochud, F., Bailat, C., Devauchelle, P., & Bourhis, J. (2019). The Advantage of FLASH Radiotherapy Confirmed in Mini-pig and Cat-cancer Patients. Clinical cancer research : an official journal of the American Association for Cancer Research, 25(1), 35–42. https://doi.org/10.1158/1078-0432.CCR-17-3375

12. Venkatesulu, B. P., Sharma, A., Pollard-Larkin, J. M., Sadagopan, R., Symons, J., Neri, S., Singh, P. K., Tailor, R., Lin, S. H., & Krishnan, S. (2019). Ultra high dose rate (35 Gy/sec) radiation does not spare the normal tissue in cardiac and splenic models of lymphopenia and gastrointestinal syndrome. Scientific reports, 9(1), 17180. https://doi.org/10.1038/s41598-019-53562-y

13. Harrington K. J. (2019). Ultrahigh Dose-rate Radiotherapy: Next Steps for FLASH-RT. Clinical cancer research : an official journal of the American Association for Cancer Research, 25(1), 3–5. https://doi.org/10.1158/1078-0432.CCR-18-1796

14. DEWEY, D. L., & BOAG, J. W. (1959). Modification of the oxygen effect when bacteria are given large pulses of radiation. Nature, 183(4673), 1450–1451. https://doi.org/10.1038/1831450a0

15. Field, S. B., & Bewley, D. K. (1974). Effects of dose-rate on the radiation response of rat skin. International journal of radiation biology and related studies in physics, chemistry, and medicine, 26(3), 259–267. https://doi.org/10.1080/09553007414551221

16. Hall, E. J., & Brenner, D. J. (1991). The dose-rate effect revisited: radiobiological considerations of importance in radiotherapy. International journal of radiation oncology, biology, physics, 21(6), 1403–1414. https://doi.org/10.1016/0360-3016(91)90314-t

17. Zlobinskaya, O., Siebenwirth, C., Greubel, C., Hable, V., Hertenberger, R., Humble, N., Reinhardt, S., Michalski, D., Röper, B., Multhoff, G., Dollinger, G., Wilkens, J. J., & Schmid, T. E. (2014). The effects of ultra-high dose rate proton irradiation on growth delay in the treatment of human tumor xenografts in nude mice. Radiation research, 181(2), 177–183. https://doi.org/10.1667/RR13464.1

18. Bourhis, J., Montay-Gruel, P., Gonçalves Jorge, P., Bailat, C., Petit, B., Ollivier, J., Jeanneret-Sozzi, W., Ozsahin, M., Bochud, F., Moeckli, R., Germond, J. F., & Vozenin, M. C. (2019). Clinical translation of FLASH radiotherapy: Why and how?. Radiotherapy

and oncology : journal of the European Society for Therapeutic Radiology and Oncology, 139, 11–17. https://doi.org/10.1016/j.radonc.2019.04.008

19. Vozenin, M. C., Montay-Gruel, P., Limoli, C., & Germond, J. F. (2020). All irradiations that are ultra-high dose rate may not be FLASH: the critical importance of beam parameter characterization and in vivo validation of the FLASH effect. Radiation Research, 194(6), 571-572.

20. Montay-Gruel, P., Bouchet, A., Jaccard, M., Patin, D., Serduc, R., Aim, W., Petersson, K., Petit, B., Bailat, C., Bourhis, J., Bräuer-Krisch, E., & Vozenin, M. C. (2018). X-rays can trigger the FLASH effect: Ultra-high dose-rate synchrotron light source prevents normal brain injury after whole brain irradiation in mice. Radiotherapy and oncology : journal of the European Society for Therapeutic Radiology and Oncology, 129(3), 582–588. https://doi.org/10.1016/j.radonc.2018.08.016

21. Gao, F., Yang, Y., Zhu, H., Wang, J., Xiao, D., Zhou, Z., Dai, T., Zhang, Y., Feng, G., Li, J., Lin, B., Xie, G., Ke, Q., Zhou, K., Li, P., Shen, X., Wang, H., Yan, L., Lao, C., Shan, L., … Du, X. (2022). First demonstration of the FLASH effect with ultrahigh dose rate high-energy X-rays. Radiotherapy and oncology : journal of the European Society for Therapeutic Radiology and Oncology, 166, 44–50. https://doi.org/10.1016/j.radonc.2021.11.004

22. Wright, M. D., Romanelli, P., Bravin, A., Le Duc, G., Brauer-Krisch, E., Requardt, H., Bartzsch, S., Hlushchuk, R., Laissue, J. A., & Djonov, V. (2021). Non-conventional Ultra-High Dose Rate (FLASH) Microbeam Radiotherapy Provides Superior Normal Tissue Sparing in Rat Lung Compared to Non-conventional Ultra-High Dose Rate (FLASH) Radiotherapy. Cureus, 13(11), e19317. https://doi.org/10.7759/cureus.19317

23. Rama, N., Saha, T., Shukla, S., Goda, C., Milewski, D., Mascia, A. E., ... & Kalin, T. V. (2019). Improved tumor control through t-cell infiltration modulated by ultra-high dose rate proton FLASH using a clinical pencil beam scanning proton system. International Journal of Radiation Oncology, Biology, Physics, 105(1), S164-S165.

24. Diffenderfer, E. S., Verginadis, I. I., Kim, M. M., Shoniyozov, K., Velalopoulou, A., Goia, D., Putt, M., Hagan, S., Avery, S., Teo, K., Zou, W., Lin, A., Swisher-McClure, S., Koch, C., Kennedy, A. R., Minn, A., Maity, A., Busch, T. M., Dong, L., Koumenis, C., … Cengel, K. A. (2020). Design, Implementation, and in Vivo Validation of a Novel Proton FLASH Radiation Therapy System. International journal of radiation oncology, biology, physics, 106(2), 440–448. https://doi.org/10.1016/j.ijrobp.2019.10.049

25. Zhang, Q., Cascio, E., Li, C., Yang, Q., Gerweck, L. E., Huang, P., Gottschalk, B., Flanz, J., & Schuemann, J. (2020). FLASH Investigations Using Protons: Design of Delivery System, Preclinical Setup and Confirmation of FLASH Effect with Protons in Animal Systems. Radiation research, 194(6), 656–664. https://doi.org/10.1667/RADE-20-00068.1

26. Chabi, S., To, T., Leavitt, R., Poglio, S., Jorge, P. G., Jaccard, M., Petersson, K., Petit, B., Roméo, P. H., Pflumio, F., Vozenin, M. C., & Uzan, B. (2021). Ultra-high-dose-rate FLASH and Conventional-Dose-Rate Irradiation Differentially Affect Human Acute Lymphoblastic Leukemia and Normal Hematopoiesis. International journal of radiation oncology, biology, physics, 109(3), 819–829. https://doi.org/10.1016/j.ijrobp.2020.10.012

27. Kim, Y. E., Gwak, S. H., Hong, B. J., Oh, J. M., Choi, H. S., Kim, M. S., Oh, D., Lartey, F. M., Rafat, M., Schüler, E., Kim, H. S., von Eyben, R., Weissman, I. L., Koch, C. J., Maxim, P. G., Loo, B. W., Jr, & Ahn, G. O. (2021). Effects of Ultra-high doserate FLASH Irradiation on the Tumor Microenvironment in Lewis Lung Carcinoma: Role of Myosin Light Chain. International journal of radiation oncology, biology, physics, 109(5), 1440–1453. https://doi.org/10.1016/j.ijrobp.2020.11.012

28. Soto, L. A., Casey, K. M., Wang, J., Blaney, A., Manjappa, R., Breitkreutz, D., Skinner, L., Dutt, S., Ko, R. B., Bush, K., Yu, A. S., Melemenidis, S., Strober, S., Englemann, E., Maxim, P. G., Graves, E. E., & Loo, B. W. (2020). FLASH Irradiation Results in Reduced Severe Skin Toxicity Compared to Conventional-Dose-Rate Irradiation. Radiation research, 194(6), 618–624. https://doi.org/10.1667/RADE-20-00090

29. Velalopoulou, A., Karagounis, I. V., Cramer, G. M., Kim, M. M., Skoufos, G., Goia, D., Hagan, S., Verginadis, I. I., Shoniyozov, K., Chiango, J., Cerullo, M., Varner, K., Yao, L., Qin, L., Hatzigeorgiou, A. G., Minn, A. J., Putt, M., Lanza, M., Assenmacher, C. A., Radaelli, E., … Busch, T. M. (2021). FLASH Proton Radiotherapy Spares Normal Epithelial and Mesenchymal Tissues While Preserving Sarcoma Response. Cancer research, 81(18), 4808–4821. https://doi.org/10.1158/0008-5472.CAN-21-1500

30. Cunningham, S., McCauley, S., Vairamani, K., Speth, J., Girdhani, S., Abel, E., Sharma, R. A., Perentesis, J. P., Wells, S. I., Mascia, A., & Sertorio, M. (2021). FLASH Proton Pencil Beam Scanning Irradiation Minimizes Radiation-Induced Leg Contracture and Skin Toxicity in Mice. Cancers, 13(5), 1012. https://doi.org/10.3390/cancers13051012

31. Sørensen, B. S., Sitarz, M. K., Ankjærgaard, C., Johansen, J. G., Andersen, C. E., Kanouta, E., Grau, C., & Poulsen, P. (2022). Pencil beam scanning proton FLASH maintains tumor control while normal tissue damage is reduced in a mouse model. Radiotherapy and oncology : journal of the European Society for Therapeutic Radiology and Oncology, 175, 178–184. https://doi.org/10.1016/j.radonc.2022.05.014

32. Zhang, Q., Gerweck, L. E., Cascio, E., Yang, Q., Huang, P., Niemierko, A., Bertolet, A., Nesteruk, K. P., McNamara, A., & Schuemann, J. (2023). Proton FLASH effects on mouse skin at different oxygen tensions. Physics in medicine and biology, 68(5), 10.1088/1361-6560/acb888. https://doi.org/10.1088/1361-6560/acb888

33. Rohrer Bley, C., Wolf, F., Gonçalves Jorge, P., Grilj, V., Petridis, I., Petit, B., Böhlen, T. T., Moeckli, R., Limoli, C., Bourhis, J., Meier, V., & Vozenin, M. C. (2022). Dose- and Volume-Limiting Late Toxicity of FLASH Radiotherapy in Cats with Squamous Cell Carcinoma of the Nasal Planum and in Mini Pigs. Clinical cancer research : an official journal of the American Association for Cancer Research, 28(17), 3814–3823. https://doi.org/10.1158/1078-0432.CCR-22-0262

34. Konradsson, E., Arendt, M. L., Bastholm Jensen, K., Børresen, B., Hansen, A. E., Bäck, S., Kristensen, A. T., Munck Af Rosenschöld, P., Ceberg, C., & Petersson, K. (2021). Establishment and Initial Experience of Clinical FLASH Radiotherapy in Canine Cancer Patients. Frontiers in oncology, 11, 658004. https://doi.org/10.3389/fonc.2021.658004

35. Bourhis, J., Sozzi, W. J., Jorge, P. G., Gaide, O., Bailat, C., Duclos, F., Patin, D., Ozsahin, M., Bochud, F., Germond, J. F., Moeckli, R., & Vozenin, M. C. (2019). Treatment of a first patient with FLASH-radiotherapy. Radiotherapy and oncology : journal of the European Society for Therapeutic Radiology and Oncology, 139, 18–22. https://doi.org/10.1016/j.radonc.2019.06.019

36. Tinganelli, W., Weber, U., Puspitasari, A., Simoniello, P., Abdollahi, A., Oppermann, J., Schuy, C., Horst, F., Helm, A., Fournier, C., & Durante, M. (2022). FLASH with carbon ions: Tumor control, normal tissue sparing, and distal metastasis in a mouse osteosarcoma model. Radiotherapy and oncology : journal of the European Society for Therapeutic Radiology and Oncology, 175, 185–190. https://doi.org/10.1016/j.radonc.2022.05.003

37. Allen, B. D., Acharya, M. M., Montay-Gruel, P., Jorge, P. G., Bailat, C., Petit, B., Vozenin, M. C., & Limoli, C. (2020). Maintenance of Tight Junction Integrity in the Absence of Vascular Dilation in the Brain of Mice Exposed to Ultra-High-Dose-Rate FLASH Irradiation. Radiation research, 194(6), 625–635. https://doi.org/10.1667/RADE-20-00060.1

38. Zhu, H., Xie, D., Yang, Y., Huang, S., Gao, X., Peng, Y., Wang, B., Wang, J., Xiao, D., Wu, D., Li, C., Li, C., Qian, C. N., & Deng, X. (2022). Radioprotective effect of X-ray abdominal FLASH irradiation: Adaptation to oxidative damage and inflammatory response may be benefiting factors. Medical physics, 49(7), 4812–4822. https://doi.org/10.1002/mp.15680

39. Ruan, J. L., Lee, C., Wouters, S., Tullis, I., Verslegers, M., Mysara, M., Then, C. K., Smart, S. C., Hill, M. A., Muschel, R. J., Giaccia, A. J., Vojnovic, B., Kiltie, A. E., & Petersson, K. (2021). Irradiation at Ultra-High (FLASH) Dose Rates Reduces Acute Normal Tissue Toxicity in the Mouse Gastrointestinal System. International journal of radiation oncology, biology, physics, 111(5), 1250–1261. https://doi.org/10.1016/j.ijrobp.2021.08.004

40. Levy, K., Natarajan, S., Wang, J., Chow, S., Eggold, J. T., Loo, P. E., Manjappa, R., Melemenidis, S., Lartey, F. M., Schüler, E., Skinner, L., Rafat, M., Ko, R., Kim, A., H Al-Rawi, D., von Eyben, R., Dorigo, O., Casey, K. M., Graves, E. E., Bush, K., … Rankin, E. B. (2020). Abdominal FLASH irradiation reduces radiation-induced gastrointestinal toxicity for the treatment of ovarian cancer in mice. Scientific reports, 10(1), 21600. https://doi.org/10.1038/s41598-020-78017-7

41. Loo, B. W., Schuler, E., Lartey, F. M., Rafat, M., King, G. J., Trovati, S., ... & Maxim, P. G. (2017). (P003) delivery of ultra-rapid flash radiation therapy and demonstration of normal tissue sparing after abdominal irradiation of mice. International journal of radiation oncology, biology, physics, 98(2), E16.

42. Eggold, J. T., Chow, S., Melemenidis, S., Wang, J., Natarajan, S., Loo, P. E., Manjappa, R., Viswanathan, V., Kidd, E. A., Engleman, E., Dorigo, O., Loo, B. W., & Rankin, E. B. (2022). Abdominopelvic FLASH Irradiation Improves PD-1 Immune Checkpoint Inhibition in Preclinical Models of Ovarian Cancer. Molecular cancer therapeutics, 21(2), 371–381. https://doi.org/10.1158/1535-7163.MCT-21-0358

43. Kim, M. M., Verginadis, I. I., Goia, D., Haertter, A., Shoniyozov, K., Zou, W., Maity, A., Busch, T. M., Metz, J. M., Cengel, K. A., Dong, L., Koumenis, C., & Diffenderfer, E. S. (2021). Comparison of FLASH Proton Entrance and the Spread-Out Bragg Peak Dose Regions in the Sparing of Mouse Intestinal Crypts and in a Pancreatic Tumor Model. Cancers, 13(16), 4244. https://doi.org/10.3390/cancers13164244

44. Evans, T., Cooley, J., Wagner, M., Yu, T., & Zwart, T. (2021). Demonstration of the FLASH Effect Within the Spread-out Bragg Peak After Abdominal Irradiation of Mice. International journal of particle therapy, 8(4), 68–75. https://doi.org/10.14338/IJPT-20-00095

45. Ferlay, J., Colombet, M., Soerjomataram, I., Mathers, C., Parkin, D. M., Piñeros, M., Znaor, A., & Bray, F. (2019). Estimating the global cancer incidence and mortality in 2018: GLOBOCAN sources and methods. International journal of cancer, 144(8), 1941–1953. https://doi.org/10.1002/ijc.31937

46. Matulonis, U. A., Sood, A. K., Fallowfield, L., Howitt, B. E., Sehouli, J., & Karlan, B. Y. (2016). Ovarian cancer. Nature reviews. Disease primers, 2, 16061. https://doi.org/10.1038/nrdp.2016.61

47. Balentova, S., & Adamkov, M. (2015). Molecular, Cellular and Functional Effects of Radiation-Induced Brain Injury: A Review. International journal of molecular sciences, 16(11), 27796–27815. https://doi.org/10.3390/ijms161126068

48. Johannesen, T. B., Lien, H. H., Hole, K. H., & Lote, K. (2003). Radiological and clinical assessment of long-term brain tumour survivors after radiotherapy. Radiotherapy and oncology : journal of the European Society for Therapeutic Radiology and Oncology, 69(2), 169–176. https://doi.org/10.1016/s0167-8140(03)00192-0

49. Butler, J. M., Rapp, S. R., & Shaw, E. G. (2006). Managing the cognitive effects of brain tumor radiation therapy. Current treatment options in oncology, 7(6), 517–523. https://doi.org/10.1007/s11864-006-0026-5

50. Caceres, L. G., Cid, M. P., Uran, S. L., Zorrilla Zubilete, M. A., Salvatierra, N. A., & Guelman, L. R. (2013). Pharmacological alterations that could underlie radiation-induced changes in associative memory and anxiety. Pharmacology, biochemistry, and behavior, 111, 37–43. https://doi.org/10.1016/j.pbb.2013.08.004

51. Meyers, C. A., Hess, K. R., Yung, W. K., & Levin, V. A. (2000). Cognitive function as a predictor of survival in patients with recurrent malignant glioma. Journal of clinical oncology : official journal of the American Society of Clinical Oncology, 18(3), 646–650. https://doi.org/10.1200/JCO.2000.18.3.646

52. Wellisch, D. K., Kaleita, T. A., Freeman, D., Cloughesy, T., & Goldman, J. (2002). Predicting major depression in brain tumor patients. Psycho-oncology, 11(3), 230–238. https://doi.org/10.1002/pon.562

53. Alaghband, Y., Cheeks, S. N., Allen, B. D., Montay-Gruel, P., Doan, N. L., Petit, B., Jorge, P. G., Giedzinski, E., Acharya, M. M., Vozenin, M. C., & Limoli, C. L. (2020). Neuroprotection of Radiosensitive Juvenile Mice by Ultra-High Dose Rate FLASH Irradiation. Cancers, 12(6), 1671. https://doi.org/10.3390/cancers12061671

54. Montay-Gruel, P., Petersson, K., Jaccard, M., Boivin, G., Germond, J. F., Petit, B., Doenlen, R., Favaudon, V., Bochud, F., Bailat, C., Bourhis, J., & Vozenin, M. C. (2017). Irradiation in a flash: Unique sparing of memory in mice after whole brain irradiation with dose rates above 100Gy/s. Radiotherapy and oncology : journal of the European Society for Therapeutic Radiology and Oncology, 124(3), 365–369. https://doi.org/10.1016/j.radonc.2017.05.003

55. Tomé, W. A., Gökhan, Ş., Brodin, N. P., Gulinello, M. E., Heard, J., Mehler, M. F., & Guha, C. (2015). A mouse model replicating hippocampal sparing cranial irradiation in humans: A tool for identifying new strategies to limit neurocognitive decline. Scientific reports, 5, 14384. https://doi.org/10.1038/srep14384

56. Montay-Gruel, P., Acharya, M. M., Petersson, K., Alikhani, L., Yakkala, C., Allen, B. D., Ollivier, J., Petit, B., Jorge, P. G., Syage, A. R., Nguyen, T. A., Baddour, A., Lu, C., Singh, P., Moeckli, R., Bochud, F., Germond, J. F., Froidevaux, P., Bailat, C., Bourhis, J., … Limoli, C. L. (2019). Long-term neurocognitive benefits of FLASH radiotherapy driven by reduced reactive oxygen species. Proceedings of the National Academy of Sciences of the United States of America, 116(22), 10943–10951. https://doi.org/10.1073/pnas.1901777116

57. Simmons, D. A., Lartey, F. M., Schüler, E., Rafat, M., King, G., Kim, A., Ko, R., Semaan, S., Gonzalez, S., Jenkins, M., Pradhan, P., Shih, Z., Wang, J., von Eyben, R.,

Graves, E. E., Maxim, P. G., Longo, F. M., & Loo, B. W., Jr (2019). Reduced cognitive deficits after FLASH irradiation of whole mouse brain are associated with less hippocampal dendritic spine loss and neuroinflammation. Radiotherapy and oncology : journal of the European Society for Therapeutic Radiology and Oncology, 139, 4–10. https://doi.org/10.1016/j.radonc.2019.06.006

58. Montay-Gruel, P., Markarian, M., Allen, B. D., Baddour, J. D., Giedzinski, E., Jorge, P. G., Petit, B., Bailat, C., Vozenin, M. C., Limoli, C., & Acharya, M. M. (2020). Ultra-High-Dose-Rate FLASH Irradiation Limits Reactive Gliosis in the Brain. Radiation research, 194(6), 636–645. https://doi.org/10.1667/RADE-20-00067.1

59. Smee, R. I., Williams, J. R., De-Loyde, K. J., Meagher, N. S., & Cohn, R. (2012). Medulloblastoma: progress over time. Journal of medical imaging and radiation oncology, 56(2), 227–234. https://doi.org/10.1111/j.1754-9485.2012.02349.x

60. Louis, D. N., Perry, A., Reifenberger, G., von Deimling, A., Figarella-Branger, D., Cavenee, W. K., Ohgaki, H., Wiestler, O. D., Kleihues, P., & Ellison, D. W. (2016). The 2016 World Health Organization Classification of Tumors of the Central Nervous System: a summary. Acta neuropathologica, 131(6), 803–820. https://doi.org/10.1007/s00401-016-1545-1

61. Udaka, Y. T., & Packer, R. J. (2018). Pediatric Brain Tumors. Neurologic clinics, 36(3), 533–556. https://doi.org/10.1016/j.ncl.2018.04.009

62. Dokic, I., Meister, S., Bojcevski, J., Tessonnier, T., Walsh, D., Knoll, M., Mein, S., Tang, Z., Vogelbacher, L., Rittmueller, C., Moustafa, M., Krunic, D., Brons, S., Haberer, T., Debus, J., Mairani, A., & Abdollahi, A. (2022). Neuroprotective Effects of Ultra-High Dose Rate FLASH Bragg Peak Proton Irradiation. International journal of radiation oncology, biology, physics, 113(3), 614–623. https://doi.org/10.1016/j.ijrobp.2022.02.020

63. Montay-Gruel, P., Acharya, M. M., Gonçalves Jorge, P., Petit, B., Petridis, I. G., Fuchs, P., Leavitt, R., Petersson, K., Gondré, M., Ollivier, J., Moeckli, R., Bochud, F., Bailat, C., Bourhis, J., Germond, J. F., Limoli, C. L., & Vozenin, M. C. (2021). Hypofractionated FLASH-RT as an Effective Treatment against Glioblastoma that Reduces Neurocognitive Side Effects in Mice. Clinical cancer research : an official journal of the American Association for Cancer Research, 27(3), 775–784. https://doi.org/10.1158/1078-0432.CCR-20-0894

64. Cao, X., Zhang, R., Esipova, T. V., Allu, S. R., Ashraf, R., Rahman, M., Gunn, J. R., Bruza, P., Gladstone, D. J., Williams, B. B., Swartz, H. M., Hoopes, P. J., Vinogradov, S. A., & Pogue, B. W. (2021). Quantification of Oxygen Depletion During FLASH Irradiation In Vitro and In Vivo. International journal of radiation oncology, biology, physics, 111(1), 240–248. https://doi.org/10.1016/j.ijrobp.2021.03.056

65. Kacem, H., Almeida, A., Cherbuin, N., & Vozenin, M. C. (2022). Understanding the FLASH effect to unravel the potential of ultra-high dose rate irradiation. International journal of radiation biology, 98(3), 506–516. https://doi.org/10.1080/09553002.2021.2004328

66. Cooper GM. The Cell: A Molecular Approach. 2nd edition. Sunderland (MA): Sinauer Associates; 2000. The Molecular Composition of Cells. Available from: https://www.ncbi.nlm.nih.gov/books/NBK9879/

67. Hall EJ, Giaccia AJ. (2019) Radiobiology for the radiologist. Eighth edition. ed. Philadelphia: Wolters Kluwer

68. Tominaga, H., Kodama, S., Matsuda, N., Suzuki, K., & Watanabe, M. (2004). Involvement of reactive oxygen species (ROS) in the induction of genetic instability by radiation. Journal of radiation research, 45(2), 181–188. https://doi.org/10.1269/jrr.45.181

69. Pratx, G., & Kapp, D. S. (2019). Ultra-High-Dose-Rate FLASH Irradiation May Spare Hypoxic Stem Cell Niches in Normal Tissues. International journal of radiation oncology, biology, physics, 105(1), 190–192. https://doi.org/10.1016/j.ijrobp.2019.05.030

70. Pratx, G., & Kapp, D. S. (2019). A computational model of radiolytic oxygen depletion during FLASH irradiation and its effect on the oxygen enhancement ratio. Physics in medicine and biology, 64(18), 185005. https://doi.org/10.1088/1361-6560/ab3769

71. Weiss, H., Epp, E. R., Heslin, J. M., Ling, C. C., & Santomasso, A. (1974). Oxygen depletion in cells irradiated at ultra-high dose-rates and at conventional dose-rates. International journal of radiation biology and related studies in physics, chemistry, and medicine, 26(1), 17–29. https://doi.org/10.1080/09553007414550901

72. Papa, S., Martino, P. L., Capitanio, G., Gaballo, A., De Rasmo, D., Signorile, A., & Petruzzella, V. (2012). The oxidative phosphorylation system in mammalian mitochondria. Advances in experimental medicine and biology, 942, 3–37. https://doi.org/10.1007/978-94-007-2869-1_1

73. Siekevitz, P. (1957). Powerhouse of the cell. Scientific American, 197(1), 131-144.

74. Nolfi-Donegan, D., Braganza, A., & Shiva, S. (2020). Mitochondrial electron transport chain: Oxidative phosphorylation, oxidant production, and methods of measurement. Redox biology, 37, 101674. https://doi.org/10.1016/j.redox.2020.101674

75. Srinivasan, S., Guha, M., Kashina, A., & Avadhani, N. G. (2017). Mitochondrial dysfunction and mitochondrial dynamics-The cancer connection. Biochimica et biophysica acta. Bioenergetics, 1858(8), 602–614. https://doi.org/10.1016/j.bbabio.2017.01.004

76. Lee, H., & Yoon, Y. (2016). Mitochondrial fission and fusion. Biochemical Society transactions, 44(6), 1725–1735. https://doi.org/10.1042/BST20160129

77. Cardanho-Ramos, C., Faria-Pereira, A., & Morais, V. A. (2020). Orchestrating mitochondria in neurons: Cytoskeleton as the conductor. Cytoskeleton (Hoboken, N.J.), 77(3-4), 65–75. https://doi.org/10.1002/cm.21585

78. Kam, W. W., & Banati, R. B. (2013). Effects of ionizing radiation on mitochondria. Free radical biology & medicine, 65, 607–619. https://doi.org/10.1016/j.freeradbiomed.2013.07.024

79. Csordás, G., & Hajnóczky, G. (2009). SR/ER-mitochondrial local communication: calcium and ROS. Biochimica et biophysica acta, 1787(11), 1352–1362. https://doi.org/10.1016/j.bbabio.2009.06.004

80. Knott, A. B., & Bossy-Wetzel, E. (2008). Impairing the mitochondrial fission and fusion balance: a new mechanism of neurodegeneration. Annals of the New York Academy of Sciences, 1147, 283–292. https://doi.org/10.1196/annals.1427.030

81. Moon, E. J., Petersson, K., & Olcina, M. M. (2022). The importance of hypoxia in radiotherapy for the immune response, metastatic potential and FLASH-RT. International journal of radiation biology, 98(3), 439–451. https://doi.org/10.1080/09553002.2021.1988178

82. Krishna, S., Arrojo E Drigo, R., Capitanio, J. S., Ramachandra, R., Ellisman, M., & Hetzer, M. W. (2021). Identification of long-lived proteins in the mitochondria reveals increased stability of the electron transport chain. Developmental cell, 56(21), 2952–2965.e9. https://doi.org/10.1016/j.devcel.2021.10.008

83. Gonzalez, S., Fernando, R., Berthelot, J., Perrin-Tricaud, C., Sarzi, E., Chrast, R., Lenaers, G., & Tricaud, N. (2015). In vivo time-lapse imaging of mitochondria in healthy and diseased peripheral myelin sheath. Mitochondrion, 23, 32–41. https://doi.org/10.1016/j.mito.2015.05.004

84. Danese, A., Patergnani, S., Bonora, M., Wieckowski, M. R., Previati, M., Giorgi, C., & Pinton, P. (2017). Calcium regulates cell death in cancer: Roles of the mitochondria and mitochondria-associated membranes (MAMs). Biochimica et biophysica acta. Bioenergetics, 1858(8), 615–627. https://doi.org/10.1016/j.bbabio.2017.01.003

85. Wang, Y., Xu, Y., Zhou, K., Zhang, S., Wang, Y., Li, T., Xie, C., Zhang, X., Song, J., Wang, X., & Zhu, C. (2022). Autophagy Inhibition Reduces Irradiation-Induced Subcortical White Matter Injury Not by Reducing Inflammation, but by Increasing Mitochondrial Fusion and Inhibiting Mitochondrial Fission. Molecular neurobiology, 59(2), 1199–1213. https://doi.org/10.1007/s12035-021-02653-x

86. Bomba-Warczak, E., & Savas, J. N. (2022). Long-lived mitochondrial proteins and why they exist. Trends in cell biology, 32(8), 646–654. https://doi.org/10.1016/j.tcb.2022.02.001

87. Mandavilli, B. S., Santos, J. H., & Van Houten, B. (2002). Mitochondrial DNA repair and aging. Mutation Research/Fundamental and Molecular Mechanisms of Mutagenesis, 509(1-2), 127-151.

88. Moehle, E. A., Shen, K., & Dillin, A. (2019). Mitochondrial proteostasis in the context of cellular and organismal health and aging. The Journal of biological chemistry, 294(14), 5396–5407. https://doi.org/10.1074/jbc.TM117.000893

89. Youle, R. J., & van der Bliek, A. M. (2012). Mitochondrial fission, fusion, and stress. Science (New York, N.Y.), 337(6098), 1062–1065. https://doi.org/10.1126/science.1219855

90. Lee, H., Smith, S. B., Sheu, S. S., & Yoon, Y. (2020). The short variant of optic atrophy 1 (OPA1) improves cell survival under oxidative stress. The Journal of biological chemistry, 295(19), 6543–6560. https://doi.org/10.1074/jbc.RA119.010983

91. Ehses, S., Raschke, I., Mancuso, G., Bernacchia, A., Geimer, S., Tondera, D., Martinou, J. C., Westermann, B., Rugarli, E. I., & Langer, T. (2009). Regulation of OPA1 processing and mitochondrial fusion by m-AAA protease isoenzymes and OMA1. The Journal of cell biology, 187(7), 1023–1036. https://doi.org/10.1083/jcb.200906084

92. Korwitz, A., Merkwirth, C., Richter-Dennerlein, R., Tröder, S. E., Sprenger, H. G., Quirós, P. M., López-Otín, C., Rugarli, E. I., & Langer, T. (2016). Loss of OMA1 delays neurodegeneration by preventing stress-induced OPA1 processing in mitochondria. The Journal of cell biology, 212(2), 157–166. https://doi.org/10.1083/jcb.201507022

93. Spinelli, J. B., Rosen, P. C., Sprenger, H. G., Puszynska, A. M., Mann, J. L., Roessler, J. M., Cangelosi, A. L., Henne, A., Condon, K. J., Zhang, T., Kunchok, T., Lewis, C. A., Chandel, N. S., & Sabatini, D. M. (2021). Fumarate is a terminal electron acceptor in the mammalian electron transport chain. Science (New York, N.Y.), 374(6572), 1227–1237. https://doi.org/10.1126/science.abi7495

94. Bacioglu, M., Maia, L. F., Preische, O., Schelle, J., Apel, A., Kaeser, S. A., Schweighauser, M., Eninger, T., Lambert, M., Pilotto, A., Shimshek, D. R., Neumann, U., Kahle, P. J., Staufenbiel, M., Neumann, M., Maetzler, W., Kuhle, J., & Jucker, M. (2016). Neurofilament Light Chain in Blood and CSF as Marker of Disease Progression in Mouse Models and in Neurodegenerative Diseases. Neuron, 91(1), 56–66. https://doi.org/10.1016/j.neuron.2016.05.018

95. Kalm, M., Abel, E., Wasling, P., Nyman, J., Hietala, M. A., Bremell, D., ... & Zetterberg, H. (2014). Neurochemical evidence of potential neurotoxicity after

prophylactic cranial irradiation. International Journal of Radiation Oncology* Biology* Physics, 89(3), 607-614.

96. Próchnicki, T., Vasconcelos, M. B., Robinson, K. S., Mangan, M. S. J., De Graaf, D., Shkarina, K., Lovotti, M., Standke, L., Kaiser, R., Stahl, R., Duthie, F. G., Rothe, M., Antonova, K., Jenster, L. M., Lau, Z. H., Rösing, S., Mirza, N., Gottschild, C., Wachten, D., Günther, C., … Latz, E. (2023). Mitochondrial damage activates the NLRP10 inflammasome. Nature immunology, 24(4), 595–603. https://doi.org/10.1038/s41590-023-01451-y